Taylor & Francis
Taylor & Francis Group

ORIGINAL RESEARCH

ə OPEN ACCESS Check for updates

AAV-mediated gene transfer of a checkpoint inhibitor in combination with HER2-targeted CAR-NK cells as experimental therapy for glioblastoma

M.I. Strecker[a,b,c], K. Wlotzka[a,b,c], F. Strassheimer[a,b,c], B. Roller[a,b,c], G. Ludmirski[a,b,c], S. König[a,b,c], J. Röder[c,d], C. Opitz[e], T. Alekseeva[c,d], J. Reul[f], L. Sevenich[b,c,d], T. Tonn[e,g], W.S. Wels[b,c,d], J.P. Steinbach[a,b,c], C.J. Buchholz[c,f,h], and M.C. Burger [ID][a,b,c]

aSenckenberg Institute of Neurooncology, Goethe University, Frankfurt, Germany; bGerman Cancer Consortium (DKTK), partner site Frankfurt/Mainz, Frankfurt, Germany; cFrankfurt Cancer Institute, Goethe University, Frankfurt, Germany; dGeorg-Speyer-Haus, Institute for Tumor Biology and Experimental Therapy, Frankfurt, Germany; eInstitute for Transfusion Medicine, German Red Cross Blood Donation Service North-East and Medical Faculty Carl Gustav Carus, TU Dresden, Dresden, Germany; fPaul-Ehrlich-Institut, Molecular Biotechnology and Gene Therapy, Langen, Germany; gGerman Cancer Consortium (DKTK), partner site Dresden, Dresden, Germany; hGerman Cancer Consortium (DKTK), partner site Heidelberg, Heidelberg, Germany

ABSTRACT

Glioblastoma (GB) is the most common primary brain tumor, which is characterized by low immunogenicity of tumor cells and prevalent immunosuppression in the tumor microenvironment (TME). Targeted local combination immunotherapy is a promising strategy to overcome these obstacles. Here, we evaluated tumor-cell specific delivery of an anti-PD-1 immunoadhesin (aPD-1) via a targeted adeno-associated viral vector (AAV) as well as HER2-specific NK-92/5.28.z (anti-HER2.CAR/NK-92) cells as components for a combination immunotherapy. In co-culture experiments, target-activated anti-HER2. CAR/NK-92 cells modified surrounding tumor cells and bystander immune cells by triggering the release of inflammatory cytokines and upregulation of PD-L1. Tumor cell-specific delivery of aPD-1 was achieved by displaying a HER2-specific designed ankyrin repeat protein (DARPin) on the AAV surface. HER2-AAV mediated gene transfer into GB cells correlated with HER2 expression levels, without inducing anti-viral responses in transduced cells. Furthermore, AAV-transduction did not interfere with anti-HER2.CAR/NK-92 cell-mediated tumor cell lysis. After selective transduction of HER2+ cells, aPD-1 expression was detected at the mRNA and protein level. The aPD-1 immunoadhesin was secreted in a time-dependent manner, bound its target on PD-1-expressing cells and was able to re-activate T cells by efficiently disrupting the PD-1/PD-L1 axis. Moreover, high intratumoral and low systemic aPD-1 concentrations were achieved following local injection of HER2-AAV into orthotopic tumor grafts *in vivo*. aPD-1 was selectively produced in tumor tissue and could be detected up to 10 days after a single HER2-AAV injection. In subcutaneous GL261-HER2 and Tu2449-HER2 immunocompetent mouse models, administration of the combination therapy significantly prolonged survival, including complete tumor control in several animals in the GL261-HER2 model. In summary, local therapy with aPD-1 encoding HER2-AAVs in combination with anti-HER2.CAR/NK-92 cells may be a promising novel strategy for GB immunotherapy with the potential to enhance efficacy and reduce systemic side effects of immune-checkpoint inhibitors.

Introduction

Glioblastoma (GB) is the most aggressive and fatal intracranial primary malignancy with an abysmal median survival of only 14.6 months.[1] Despite tremendous research efforts, broad molecular characterization and the optimization of multimodal therapy interventions such as surgery, radiotherapy and systemic therapy (chemotherapy, targeted therapy), the relapse rate of GB is high, and the lack of effective treatment options upon recurrence results in a poor overall prognosis.[2,3] Consequently, there have been considerable efforts to explore more advanced therapeutic options including immunotherapy. In recent years, precision oncology employing immune-checkpoint inhibitors (ICIs) and combination immunotherapies has led to promising clinical outcomes for a variety of tumor entities. However, initial clinical trial results on

immunotherapy of GB have been disappointing, presumably due to challenges such as persistent immunosuppression and pronounced T-cell dysfunction. To specifically target HER2+ GB cells, we previously generated a HER2-specific clonal derivative of the clinically applicable NK-92 cell line (NK-92/5.28.z, for clarity hereafter in some instances also termed "anti-HER2. CAR/NK-92").[4,5] The cells express a chimeric antigen receptor based on the HER2-specific antibody FRP5 fused to CD28 and CD3ζ signaling domains. Similar to other malignancies of solid tumor origin, a large proportion of glioblastomas are HER2+. HER2 protein expression was found in up to 80% of GB tumors and was correlated with impaired survival.[6–9] HER2 RNA expression also in normal brain tissue has been shown by the Human Proteome Map, both in bulk RNA and single cell sequencing data.[10] We have previously investigated HER2 protein expression with immunohistochemistry in glioblastomas

and found in a high proportion of tumors increased expression of HER2 as compared to adjacent non-neoplastic tissue.[5] It has been demonstrated before that high and specific lytic activity of anti-HER2.CAR/NK-92 against HER2$^+$ GB cells can be achieved *in vitro*. Additionally, repetitive intratumoral injection of anti-HER2.CAR/NK-92 cells significantly prolonged symptom-free survival in murine orthotopic xenograft models. Furthermore, activation of an endogenous immune response by anti-HER2.CAR/NK-92 treatment has been shown to be instrumental for rejection of tumors in the syngeneic GL261-HER2 model.[5] Based on these results, we initiated the ongoing first-in-human phase I clinical study CAR2BRAIN for patients with relapsed HER2-positive GB (NCT03383978, clinicaltrials.gov).[11,12] Following successful completion of single-dose dose escalation, we are currently evaluating safety and feasibility of repetitive local injections of anti-HER2.CAR/NK-92 cells in the expansion cohort of the trial.[12] In preclinical models, anti-HER2.CAR/NK-92 treatment induced rejection of small tumors in the GL261-HER2 model,[5] and combination with systemic application of a PD-1-specific antibody restored efficient anti-tumor responses even in more advanced stages.[13] Translating this into the clinical setting, we included an additional patient cohort in the CAR2BRAIN study that receives a combination therapy with anti-HER2.CAR/NK-92 and anti-PD-1 checkpoint inhibition.

NK-92 cells functionally resemble activated primary NK cells in several aspects. NK-92 express many activating NK receptors such as NKp30, NKp46 and NKG2D, but lacks most inhibitory NK receptors except KIR2DL4, Ig-like transcript 2 (ILT-2) and NKG2A/C94.[14–16] NK-92 cells were originally derived from a non-Hodgkin lymphoma,[17] and in ongoing clinical trials are irradiated with 10 Gy prior to transfusion to exclude the risk of secondary lymphoma formation.[18] This limits their functional activity to a maximum of 72 h.[19] In NK cells obtained from donor blood or umbilical cord blood, no prophylactic irradiation would be necessary, expected to prolong the time period of activity. In contrast to donor blood or umbilical cord derived NK cells, NK-92 cells do not express CD16 and thus cannot mediate ADCC.[20]

The core obstacle of immunotherapy in glioma is the immunosuppressive microenvironment, which together with the comparatively low mutational burden and therefore low immunogenicity prevents an effective immune response.[21,22] In GB both, tumor cells and monocytes/macrophages express PD-L1, which blocks CD8$^+$ and CD4$^+$ T-cell activation.[23,24] Therefore, immunotherapy with ICIs directed against the PD-1/PD-L1 axis is a promising approach for GB treatment. Indeed, in a study involving 35 patients, the anti-PD-1 antibody pembrolizumab increased survival in the neoadjuvant setting.[25] However, several randomized trials exploring ICI monotherapy in adjuvant and recurrent settings have failed to meet their primary endpoint.[26] Additionally, the occurrence of immune-related adverse events limits the applicability of systemic ICIs, and represents an obstacle in particular toward the development of combination immunotherapies.[27] By local or systemic injection of adeno-associated viral vectors (AAVs), local expression and secretion of ICIs after the transduction of tumor cells *in vivo* becomes feasible.[28] Cargo gene expression limited to the tumor area allows for high intratumoral and low

systemic drug concentrations. While none of the natural AAV serotypes are specific for malignant cells,[29] genetic fusion of a viral capsid protein (VP2) to designed ankyrin repeat proteins (DARPins), which are highly specific genetically engineered proteins designed to mimic antibodies, allows for the generation of AAVs with specificity for HER2$^+$ cells.[30–32] By selectively transducing HER2$^+$ tumor cells, such HER2-AAVs induce the secretion of an encoded anti-PD-1 immunoadhesin (aPD-1) into the tumor microenvironment (TME). This approach might facilitate the modulation of the immunosuppressive TME by disruption of the PD-1/PD-L1 axis and thereby also mediate synergistic effects when combined with anti-HER2.CAR/NK-92 cell therapy.

In this study, we evaluated the functional characteristics and immune-modulating effects of both, HER2-targeted anti-HER2.CAR/NK-92 cells, and HER2-AAV, which induce the expression of aPD-1. We addressed the influence of target-activated anti-HER2.CAR/NK-92 cells on tumor cells and bystander immune cells as well as HER2-AAV transduction efficacy and functionality of the secreted aPD-1 *in vitro*. Furthermore, we investigated the characteristics and distribution kinetics of the HER2-targeted AAV in LN-319 human glioblastoma xenograft and syngeneic GL261-HER2 glioblastoma mouse models *in vivo*. We assessed whether the modified AAV vector triggers host immune reactions such as the generation of neutralizing antibodies (nAbs) or the production of inflammatory cytokines and generated data critical for the future application of anti-HER2.CAR/NK-92 cells and aPD-1 encoding HER2-AAV as a novel combination immunotherapy approach.

Materials and methods

Cell culture

Established human LN-319 glioblastoma cells (kindly provided by Monika Hegi, Lausanne, Switzerland), human U138MG glioblastoma cells (kindly provided by N. de Trebolet, Lausanne, Switzerland), LNT-229 cells expressing EGFRvIII[33] as well as murine GL261 glioblastoma cells, immortalized murine microglia BV2, immortalized human microglia C20 and HMC3, human fibrosarcoma cells HT1080 (ATCC CCL-121) and immortalized human astrocytes NHA-E6/E7/hTERT (abbreviated as "NHA" thereafter for brevity)[34] were cultured in Dulbecco´s modified Eagle´s medium (DMEM, Gibco, Darmstadt, Germany) containing 10% fetal calf serum (FCS; Biochrom KG, Berlin, Germany), 100 IU/ml penicillin and 100 µg/ml streptomycin (Life Technologies, Karlsruhe, Germany) in cell culture incubators at 37°C and 5% CO_2. HER2$^+$ murine glioma cell lines GL261-HER2, Tu2449-HER2 and Tu9648-HER2 were generated by lentiviral transduction with the human antigen. HER2-overexpressing LN-319-HER2 cells were generated by stably transfecting endogenously HER2$^+$ LN-319 cells with a pcDNA3-HER2 plasmid.[5] The immortalized murine microglia cell line EOC2 was cultured in DMEM with 2 mM L-glutamine supplemented with IL-34 (20 ng/ml) and TGF-β (5 ng/ml). NK-92 WT, as well as NK-92/5.28.z (anti-HER2.CAR/NK-92) NK-92/MR1-1.28.z (anti-EGFRvIII.CAR/NK-92) cells[4,35] were cultured in X–VIVO 10 medium (Lonza) supplemented with 5% heat-inactivated

human plasma (German Red Cross Blood Donation Service Baden-Württemberg – Hessen, Frankfurt am Main, Germany) and 100 U/ml IL-2 (Proleukin; Novartis Pharma, Nürnberg, Germany). Primary human glioblastoma cells MNOF-1300, MNOF-168 and MNOF-76 were grown in flasks pre-coated with 5 mg/ml laminin (Sigma-Aldrich, Taufkirchen, Germany) in DMEM/F12 medium (Lonza) containing 20 ng/ml each of recombinant epidermal growth factor (EGF) and human recombinant basic fibroblast growth factor 2 (bFGF2) (ReliaTech, Wolfenbüttel, Germany), and 20% BIT Admixture Supplement (Pelo Biotech, Planegg/Martinsried, Germany).[5] Human astrocytes (HuA) (Innoprot, Derio, Spain) were cultured in Astrocyte medium (Innoprot, Derio, Spain) according to the manufacturer's protocol. PD-1 expressing HT1080 cells (HT1080-PD-1)[28] were cultured in DMEM supplemented with 10% FCS, 2 mM L-glutamine, and 10 µg/ml puromycin.

Viral vectors

HER2-AAV[aPD−1] and HER2-AAV[IgG-Fc] have been described previously.[28]

In vitro *transduction and analyses*

Cytotoxicity assays

Cytotoxic NK-cell activity was determined using a fluorescence-activated cell scanning (FACS)-based assay as previously described.[36] Calcein violet AM (Life Technologies, Darmstadt, Germany) labeled target cells were washed and co-cultured with effector cells at different effector to target (E/T) ratios for 2 h at 37°C. Prior to flow cytometric analysis, cells were washed and resuspended in 200 µl of a propidium iodide (PI; 1 µg/ml) solution. Calcein violet AM and PI double positive cells represented dead target cells. Spontaneous target cell lysis in the absence of effector cells was substracted from the values to determine specific lysis. Data were analyzed using FlowJo™ software (Version 10.0.7; FlowJo Ashland, OR).

Transwell assays

Cytokine release as well as PD-L1 regulation in tumor and immune cells was determined in transwell cytotoxicity assays using ThinCert™ cell culture inserts (Greiner Bio-One, Frickenhausen, Germany). Cells of interest were seeded into the wells of a 24 well plate at a density of 5×10^4 cells per well. A cytotoxicity assay was performed in the insert for 24 h, before the insert was removed and the culture medium in the base was replaced by serum-free DMEM. Human as well as murine recombinant IFN-γ as a positive control for PD-L1 upregulation and cell stimulation was used at a concentration of 100 ng/ml. Stimulated cells in the base were cultivated for 24 h, then the conditioned medium was harvested, centrifuged, filtered and stored at −80°C until analysis.

Flow cytometry

Expression of HER2 on the surface of GL261-HER2, Tu2449-HER2, Tu9648-HER2 and LN-319 cells was determined by flow cytometry using AlexaFluor® 647 anti-human HER2 antibody 24D2 (BioLegend, Fell, Germany). Presence of mutated EGFRvIII on the surface of LNT-229-EGFRvIII cells was analyzed using an AlexaFluor® 488 anti-EGFR mutant antibody DH8.3 (Novus Biologicals). CAR expression of anti-HER2. CAR/NK-92 cells was analyzed using a HER2-Fc fusion protein (R&D Systems, Wiesbaden-Nordenstadt, Germany) followed by APC-coupled goat anti-human antibody (Dianova, Hamburg, Germany). PD-L1 expression by murine and human cells was determined using APC-coupled anti-mouse or anti-human PD-L1 antibodies, respectively. Cell viability was analyzed by propidium iodide uptake as previously described.[37] A FACSCanto II flow cytometer was used for flow cytometric analyses (BD Biosciences, Heidelberg, Germany), and data were evaluated using FlowJo™ software. For cell sorting, a FACSAria flow cytometer was used (BD Biosciences).

In vitro *transduction experiments*

Transgene expression in HER2^{+} target cells was assessed *in vitro* upon transduction with HER2-AAV[aPD−1] and HER2-AAV[IgG-Fc] vectors as described before.[28] Briefly, tumor cells were grown in 96-, 24- or 12-well plates at a cell density of 8×10^3, 5×10^4 or 8×10^4 cells/well, respectively, prior to incubation with AAV particles (≥450,000 genome copies/cell). After 24 h, cells were washed in PBS, and serum-free medium (virus production serum free medium (VPSFM), Thermo Fisher Scientific, Dreieich, Germany) was added. Cells were cultured for 4 days before harvested media were centrifuged at 300 x g for 5–7 min and stored at 4°C (or −80°C for long-term storage) before aPD-1 release was determined by Western blot and quantified by ELISA.

Western blot

For Western blot analyses, supernatants from GL261 cultures were denatured at 95°C in Laemmli buffer containing SDS, β-mercaptoethanol and dithiothreitol (DTT). Proteins were separated via SDS-PAGE in a 12% polyacrylamide gel and transferred onto nitrocellulose membranes using a semi-dry blot system (BioRad, Feldkirchen, Germany). AAV-encoded murine aPD-1 was detected using a primary antibody specific for the HA-tag included in the molecule (mouse, clone 16B12; Abcam, Cambridge, UK). A secondary anti-mouse antibody was purchased from Santa Cruz (#sc-2020). For chemiluminescence detection, membranes were treated with Pierce™ ECL Plus Western Blotting Substrate (Thermo Fisher Scientific) prior to exposure on X-ray films.

RNA extraction and quantitative real time PCR

Following viral transduction, total RNA of GL261, Tu9648 and LN-319 cells was extracted using TRIzol and EXTRACTME RNA isolation kit (Blirt, Gdansk, Poland), then cDNA was

Table 1. Primer sequences.

Name	Sequence/Description
18s_fwd	CTACCACATCCAAGGAAG
18s_rev	GGACTCATTCCAATTACAG
aPD1_fwd	CCAAGTCCTACAACTATG
aPD1_rev	GTCCTCAGATTGTTCATC
SDHA_h_fwd	GTGCGGATTGATGAGTAC
SDHA_h_rev	CAACGTCCACATAGGACA
Sdha_m_fwd	CGACAAGACCTTGAATGA
Sdha_m_rev	GCTGTTGATCACAATCTATG

synthesized using the Vilo cDNA synthesis kit (Invitrogen, Carlsbad, CA, USA). Quantitative real time PCR (qPCR) was performed using the Absolute Blue SYBR Green Fluorescein q-PCR Mastermix (Thermo Fisher Scientific). Corresponding primer pairs for the aPD1 transgene are listed in Table 1. Gene expression values were normalized to two house-keeping genes (18S and SDHA) and values were calculated using the ΔCT method.

Cytokine measurements

Concentrations of human IFN-γ, TNF-α, MCP-1, IL-1α, IL-2, IL-8, IL-10 and perforin in cell culture supernatants were measured using ProcartaPlex Immunoassay Mix & Match panels and a Luminex FLEXMAP3D (ThermoFisher Scientific, Darmstadt, Germany). The data were analyzed using the ProcartaPlex Analyst 1.0 Software (ThermoFisher Scientific). All other cytokine concentrations in cell culture supernatant or serum samples were measured with the LEGENDplex™ Inflammation Panel and the LEGENDplex™ Anti-Virus Response Panel (Mouse & Human) Kits (BioLegend) according to the manufacturer's protocol. Briefly, diluted samples were mixed with beads in a V-bottom plate. The plate was incubated at 800 rpm on a plate shaker for 2 h at room temperature (RT). After washing, detection anti-bodies were added to each well. Samples were incubated at 800 rpm on a plate shaker for 1 h at RT and 25 μL of Streptavidin R-Phycoerythrin conjugate (SA-PE) were directly added to each well. After 30 min, the plate was washed again before samples were analyzed in 150 μl of washing buffer on a flow cytometer. For analysis, the LEGENDplex™ Data Analysis Software Suite was used.

Enzyme-linked immunosorbent assay (ELISA)

The concentration of HA-tagged AAV-encoded murine aPD-1 was measured by ELISA. 96-well immunoplates (Nunc MAxiSorp, Thermo Fisher Scientific) were coated with an anti-HA antibody (50 μl, 1:4,000 in PBS, ab9110, Abcam) at 4°C overnight in a humidified chamber. After washing (3x, 0.05% Tween20 in PBS), wells were blocked at RT for 1 h on a shaker (5% FCS, 0.05% Tween 20 in PBS), then 100 μl of prepared standard and sample (cell culture supernatant from transduced cells, mouse serum or organ lysate) were added to the wells. The plate was covered and incubated at RT for 2 h on a shaker. After washing 5x, bound aPD-1 was detected using a goat anti-mouse IgG HRP-conjugated detection antibody (1:30,000 in blocking buffer, ab97265, Abcam) and visualized using 1-StepTM Ultra TMB chromogenic substrate (Thermo Fisher

Scientific, Dreieich, Germany). Recombinant aPD-1 from transfected HEK293T cells was purified via protein A affinity chromatography and subsequently concentrated before it was used as standard in order to generate reference values.

Target binding assay

Specific target binding of AAV-encoded aPD-1 to PD-1 was assessed via flow cytometry using murine PD-1 expressing cells. 400 μl of cell culture supernatant from transduced GL261, Tu9648 or LN-319 cells were added to 5×10^4 HT1080-PD-1 cells followed by incubation at 4°C for 1 h. Binding was detected using a FITC-labeled antibody against the murine Fc part (Abcam) at 4°C for 15 min. PD-1⁻ parental HT1080 cells were used as negative control. Data were analyzed using FlowJo™ software.

Blockade assay

Functionality of murine aPD-1 was determined using a PD-1/PD-L1 Blockade Bioassay (Promega, Walldorf, Germany) according to the manufacturer's protocol. Briefly, PD-L1 expressing aAPC/CHO-K1 target cells that also harbor an engineered cell surface protein for activation of T-cell receptors (TCRs) in an antigen-independent manner were incubated with PD-1 expressing effector T cells. The effector T cells express a luciferase reporter driven by an NFAT response element. Interruption of PD-1/PD-L1 signaling by the addition of cell culture supernatant containing aPD-1 re-activates TCR signaling. This results in NFAT-mediated luciferase expression, which was detected by the addition of Bio-Glo™ reagent. Luminescence was measured using a TecanSpark Luminescence Multi Mode Microplate Reader (Tecan, Männedorf, Switzerland).

In vivo analyses

Glioblastoma mouse models

All *in vivo* experiments were carried out in accordance with the guidelines and regulations of the German animal protection law upon approval by the responsible government committee (Regierungspräsidium Darmstadt, Darmstadt, Germany, approval number FK-1088). For *in vivo* transduction and bio-distribution analyses, 6–8 weeks old female C57BL/6, B6C3F1 or Crl:NU(NCr)-Foxn1ⁿᵘ mice (Charles River Laboratories, Sulzfeld, Germany) were used for syngeneic GL261-HER2 or Tu2449-HER2 murine glioblastoma models and LN-319 human glioblastoma xenograft models, respectively. Initial analysis of aPD-1 biodistribution kinetics was performed in subcutaneous glioblastoma models. Crl:NU(NCr)-Foxn1ⁿᵘ mice were engrafted with 2×10^6 LN-319 tumor cells, C57BL/6 and B6C3F1 mice were engrafted with 1×10^6 GL261-HER2 or Tu2449-HER2 cells at the right flank, respectively. For orthotopic glioblastoma models, anesthetized mice were immobilized in a stereotaxic fixation device (Stoelting, Wood Dale, USA) and injected with 5×10^3 GL261-HER2 tumor cells in 2 μL PBS using a 10 μL Hamilton syringe (Hamilton, Bonaduz, Switzerland) and a Quintessential Stereotaxic Injector (Stoelting, Wood Dale, USA) through a burr hole in

the skull. Tumor cells were injected into the right striatum with a depth of 3 mm to the skull, at a speed of 0.5 µL/min. After 2 min, the needle was withdrawn at a speed of 1 mm/min. Tumor growth, body weight and overall health status of all animals were monitored throughout the study. For the orthotopic model, tumor growth was monitored by magnetic resonance imaging (MRI) as described below. In subcutaneous survival studies, tumor growth was monitored 3x weekly using a caliper. Tumor volume was determined using the following formula: Tumor volume (mm^3) = length (mm) x width $(mm)^2$ x 0.5. Animals were sacrificed upon weight loss of ≥20% body weight or tumor ulceration. Final endpoint of survival experiments was a tumor volume ≥1500 mm^3. HER2-AAV was injected either intratumorally or intravenously into the tail vein when tumors exceeded a pre-defined minimum volume of 30–80 mm^3, depending on the experimental setup. Each vector dose contained 1×10^{11} (subcutaneous tumors) or 3×10^{10} (intracranial tumors) genome copies (gc).

MR imaging

Tumor engraftment was determined 7 days after tumor cell injection via a 7 Tesla Small Animal MR Scanner (Pharmascan, Bruker, Berlin, Germany). Mice were injected intraperitoneally (i.p.) with 150 µl contrast agent (Gadovist, Bayer, Leverkusen, Germany), and then anesthetized with isoflurane (1.5%). During scan acquisition, respiration rate was permanently monitored. Image acquisition was performed using Paravision 6.0.1 software in coronal planes (parameters: FOV = 20x20 mm, 11 slices, 0.5 mm slice thickness, acquisition matrix = 256x256, flip angle 90°).[38]

Sample preparation and analysis

For the detection of murine aPD-1 in serum, tumor and organ tissues, mice were sacrificed via cervical dislocation at pre-specified time points (kinetic studies: day 3–10). Blood sampling was performed via heart puncture, serum was isolated upon a clotting time of 30 min and centrifugation at 5,000 rpm for 10 min. Serum samples were stored at −80°C until further analysis. Tumor tissue as well as organs (brain, heart, lung, kidney, liver, spleen) were isolated, snap frozen in liquid nitrogen and stored at −80°C. For preparation of tissue lysates, organs were thawed on ice, weighed and homogenized in 5 µl/mg lysis buffer (10 ml lysis buffer + 10 µl DNAse, + PIC (Roche)) using a TissueLyzer LT (Qiagen, Hilden, Germany) at a frequency of 50 Hz for 5 min. Cell homogenates were incubated on ice for 15 min before pelleting at 13,000 rpm for 15 min at 4°C. Supernatants were stored at −80°C until ELISA analysis.

Isolation and cultivation of splenocytes from mice

Mice were sacrificed by cervical dislocation, then spleens were isolated and dissociated using the gentleMACS Octo Dissociator (Miltenyi Biotec, Bergisch Gladbach, Germany) according to the manufacturer's protocol. The resulting single cell suspension was filtered through a 70 µm strainer and

subsequently washed with Roswell Park Memorial Institute (RPMI) medium, then cells were pelleted for 5 min at 1,600 rpm. Erythrocyte lysis was performed in 5 ml red blood cell lysis buffer for 5 min at RT. Cells were washed 2x, resuspended in 5 ml RPMI and seeded in a round-bottom 96-well plate ($5x10^5$ cells/well). For binding assays, cells were cultivated in RPMI supplemented with 2 µl/well DYNAL™ Dynabeads™ (Thermo Fisher Scientific) for 48 h.

Neutralization assay

For neutralization assays, Tu9648-HER2 cells were seeded in white 96-well-plates (Corning, Kaiserslautern, Germany) at a density of 1×10^4 cells/well and cultured in a 37°C, 5% CO_2 incubator for 24 h. The next day, murine serum samples were heat inactivated at 56°C for 30 min and diluted 1:10 in FCS. Heat inactivated human plasma and FCS were used as controls. 20 µl of sample were transferred to the wells of a 96-well U-bottom plate before HER2-AAV^{Luc} was added ($4x10^7$ gc/µl in 20 µl serum-free DMEM) to each well. Plates were incubated at 37°C and 5% CO_2 for 1 h to allow neutralization. Next, 10 µl of sample were added to the Tu9648-HER2 cells. Plates were incubated overnight before transduction was quantified with the Bright-Glo™ Luciferase Assay System (Promega) according to the manufacturer's instructions. Luminescence was determined using a Centro LB 960 microplate luminometer (Berthold Technologies, Bad Wildbad, Germany).

Schematics

Schematics were created using BioRender.com.

Statistical analysis

Quantitative data are expressed as mean and standard deviation (SD). Statistical significance was determined using a two-tailed student's t-test, if not stated otherwise. If multiple sample groups were compared, significance was determined by ANOVA test. $p < 0.05$ was regarded as statistically significant. All analyses were performed using GraphPad Prism (Version 9.1.2.226; GraphPad Software, La Jolla, CA).

Results

Anti-HER2.CAR/NK-92 cells efficiently lyse HER2⁺ cells and elicit cytokine release from the TME

Since HER2 serves as a target for both, aPD-1 encoding HER2-AAVs and anti-HER2.CAR/NK-92 cells, we first confirmed expression on murine glioma cells before and after lentiviral transduction with the human HER2 antigen in comparison to the human glioma cell line LN-319 and the primary glioma cell culture MNOF-1300 (Figure 1a). CAR expression on NK-92 cells was verified via flow cytometry (Figure S1a). Cytotoxicity depended on HER2 expression of the target cells, in accordance with our previous work[5] (Figure 1b). Since transduced murine glioma cell lines express very high HER2 levels, we also assessed anti-HER2.CAR/NK-92 cell activity on GL261-HER2-low cells that roughly reflect the HER2 level of endogenously
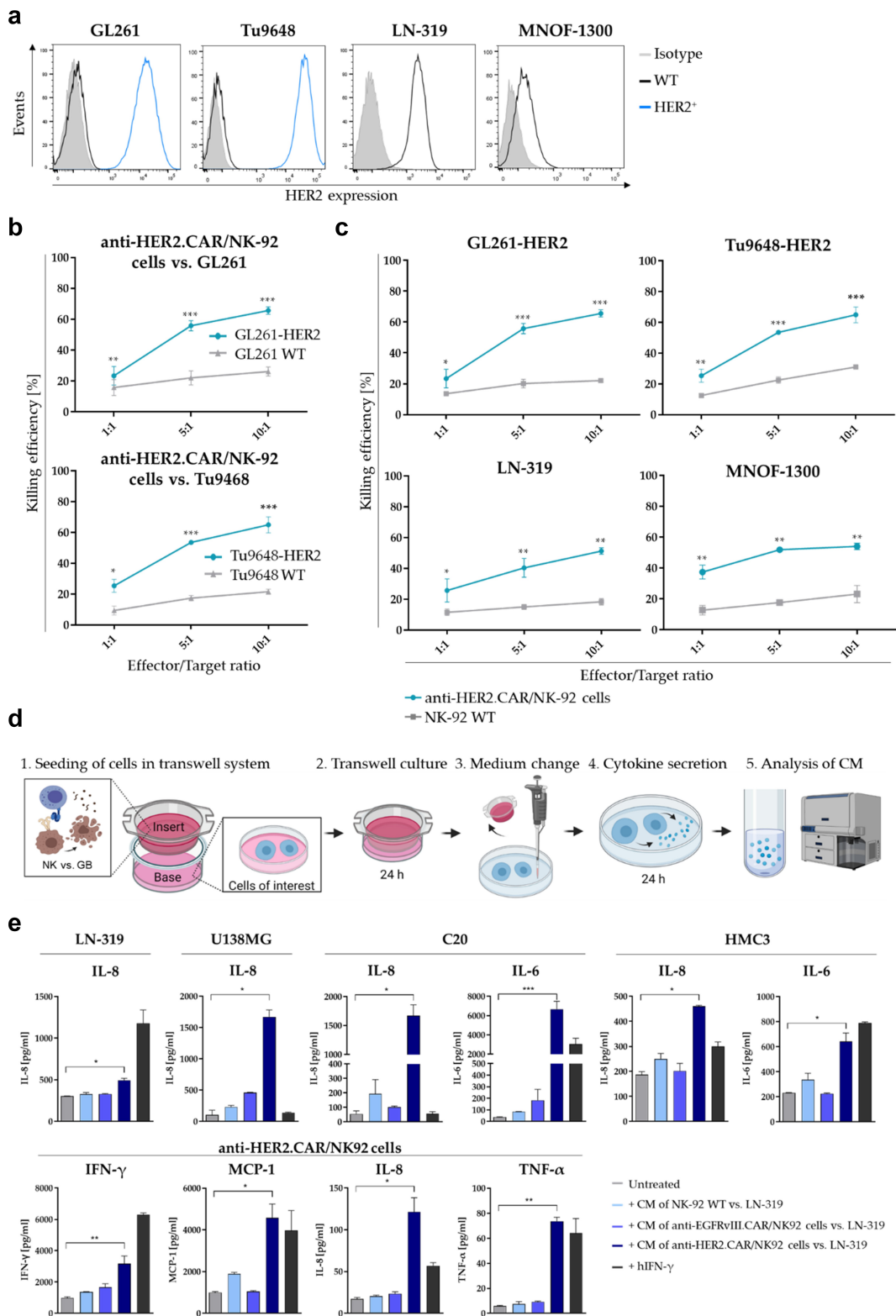
Figure 1. HER2-targeted anti-HER2.CAR/NK-92 cell therapy. (**a**) HER2 expression of murine HER2-transduced glioma cell lines (GL261, Tu9648, blue histogram), the human glioma cell line LN-319 as well as MNOF-1300 primary glioma cells as determined via flow cytometry. (**b**) Cytotoxic activity of anti-HER2.CAR/NK-92 cellsel against wild-type HER2- murine glioma cells as compared to cells transduced to express HER2 (Mean values ± SD are shown; n=3, *p < 0.05; **p < 0.01, ***p < 0.001). (**c**) Analysis of cytotoxic activity of anti-HER2.CAR/NK-92 cells against target cells of murine (top) and human (bottom) origin as compared to parental NK-92 cells (Mean values ± SD are shown; n=3, **p < 0.01; ***p < 0.001). (**d**) Schematic representation of the cytokine response transwell assay design. Soluble factors secreted from anti-HER2.CAR/NK-92 cells stimulated by glioblastoma cells (GB) in the insert influence cells of interest in the base. After 24 h of co-culture, the insert is removed and fresh serum-free medium is added to the cells in the base. Stimulated cells are cultivated for further 24 h. Cytokine levels in the conditioned medium are determined via a bead-based LEGENDplex assay. (**e**) Analysis of cytokine release by various cell types of the TME that were exposed to conditioned medium (CM) from different NK cell/tumor cell co-culture assays (E/T ratio 1:1). Co-culture in the insert consisted of NK-92 WT cells vs. LN-319 (light blue), anti-EGFRvIII.CAR/NK-92 vs. LN-319 (middle blue) and anti-HER2.CAR/NK-92 vs. LN-319 (dark blue); hIFN-γ [100ng/ml] was added to the cells as positive control for cell stimulation (black). Cells were cultivated in CM for 24 h, then cells were washed, medium was changed to serum-free medium and cytokine secretion was assessed after further 24 h using a beadbased immunoassay. Mean values ± SD are shown; n=3. *p < 0.05, **p < 0.01.

HER2^{+} cells such as LN-319 (Figure S1b) and found no difference in killing efficiency (Figure S1c and S1d). Anti-HER2. CAR/NK-92 cells had high lytic activity toward HER2^{+} target cells, and specificity was demonstrated by the low lytic activity of the parental NK-92 cell line (Figure 1c). The naturally HER2^{+} human glioma cell line LN-319 and human primary glioma cells (MNOF-1300) were both efficiently lysed by anti-HER2.CAR/NK-92 cells (Figure 1c, bottom and Figure S1e and f). As control, NK-92 cells transduced with a CAR targeting the unrelated antigen EGFRvIII (NK-92/MR1-1.28.z, for clarity hereafter also called "anti-EGFRvIII.CAR/NK-92") did not target HER2^{+} EGFRvIII^{−} cells (Figure S2a-d). Importantly, HER2 levels on target cells did not decrease upon contact with anti-HER2.CAR/NK-92 cells (Figure S2e), indicating no antigen downregulation in response to anti-HER2.CAR/NK-92 cell lysis. This is in line with previous work, where we have observed that repetitive anti-HER2.CAR/NK-92 cell therapy in animal glioblastoma models does not induce downregulation of HER2 on target cells as a conceivable escape mechanism.[5]

To characterize the effect that anti-HER2.CAR/NK-92 cell-mediated tumor cell lysis has on other cell types typically present within a tumor microenvironment (TME), we investigated whether cytokine secretion by activated anti-HER2.CAR/NK-92 cells stimulates cytokine release from human glioma cells (LN-319, U138MG) as well as from human microglia (MG) (C20, HMC3) and non-activated bystander anti-HER2. CAR/NK-92 cells. We identified a pattern of significantly increased levels of the cytokines IFN-γ, TNF-α, MCP-1, IL-8 and IL-6 (Figure 1e). The glioma cell lines LN-319 and U138MG showed increased secretion of IL-8, while in microglia (C20 and HMC3) levels of IL-6 and IL-8 were elevated. In anti-HER2.CAR/NK-92 cells, secretion of IFN-γ, MCP-1, IL-8 and TNF-α was enhanced. These data indicate a pro-inflammatory effect induced by anti-HER2.CAR/NK-92 cells on various cell types which comprise the TME. We found no significant changes in the levels of MCP-1 and IFN-α2 in LN-319 and U138MG cells (Figure S2f). Levels of IL-1β, IL-12p70, IL-17A, IL-23, and IL-33 (for all cell types evaluated), IL-6 (LN-319, U138MG, anti-HER2.CAR/NK-92), MCP-1, IFN-γ and TNF-α (LN-319, U138MG, C20, HMC3) were below the detection limit of the method (data not shown).

Anti-HER2.CAR/NK-92 cell-mediated tumor cell lysis induces IFN-γ dependent PD-L1 upregulation in different cell types

Since the PD-1/PD-L1 interaction is a decisive determinant of the immunosuppressive TME, we evaluated PD-L1 levels and their regulation in different cell types in response to anti-HER2.CAR/NK-92 cell therapy. For this, we employed a transwell system where soluble factors secreted from stimulated anti-HER2.CAR/NK-92 cells in a cell culture insert influence cells of interest in the base of a well plate (Figure 2a). Co-cultivation in the presence of anti-HER2.CAR/NK-92 cells activated by HER2^{+} tumor cells induced PD-L1 upregulation in human glioma cells, MG and astrocytes (Figure 2b and Figure S3a). Transwell cultivation of those cell types either with unstimulated anti-HER2.CAR/NK-92 cells alone or with non-activated NK cells (parental NK-92 WT cells or EGFRvIII-

specific anti-EGFRvIII.CAR/NK-92 vs. GL261-HER2 or LN-319) did not alter PD-L1 levels (Figure S3b and c). The upregulation of PD-L1 as a response to adjacent killing of glioma cells by the anti-HER2.CAR/NK-92 cells is a key finding, as the consequential activation of the PD-1/PD-L1 axis may suppress further endogenous anti-glioma immunity which has been shown to be paramount for *in vivo* efficacy of anti-HER2. CAR/NK-92 cell therapy.[5] As anti-HER2.CAR/NK-92 cells in the insert and tumor cells in the base of the transwell system are not in direct contact (Figure 2a), the effect observed is most likely induced by soluble factors secreted by anti-HER2.CAR/NK-92 cells activated upon killing of tumor cells in the insert. Murine glioma cells did not show an increase in PD-L1 levels upon co-cultivation with activated anti-HER2.CAR/NK-92 cells due to species differences in the putative mediators of the effect as the anti-HER2.CAR/NK-92 cells used are of human origin. In order to evaluate which soluble factors are associated with PD-L1 upregulation, we measured the direct cytokine response of anti-HER2.CAR/NK-92 cells activated by target cell killing. Upon co-cultivation with murine glioma cells, an increase in the levels of human IFN-γ, IL-1α, TNF-α, IL-8, MCP-1 and IL-10 and perforin was observed, while levels of IL-2 appear to decrease in response to antigen (Figure 2c). To determine whether stimulation with these cytokines induced PD-L1 upregulation in murine or human cells present in the TME, PD-L1 expression on MG, astrocytes and tumor cells was assessed via flow cytometry 24 h post treatment. Stimulation with IFN-γ increased PD-L1 expression by human cells similar to stimulation with conditioned medium from a killing assay (Figure 2d). These effects were reversed by adding anti-IFN-γ to the experimental setup, antagonizing PD-L1 upregulation upon stimulation with conditioned medium (Figure 2e). This indicates that IFN-γ acts as the major driver of PD-L1 regulation upon anti-HER2.CAR/NK-92 cell therapy.

Taken together, these data suggest that upregulation of PD-L1 not only by glioma cells but also by brain resident cell types such as MG and astrocytes could add to the immunosuppressive microenvironment and constitute a potential mechanism of resistance toward anti-HER2.CAR/NK-92 cell therapy. Consequently, we explored selective local administration of a checkpoint inhibitor through a HER2-targeted AAV vector to specifically interfere with the PD-L1/PD-1 interaction.

HER2-AAV efficiently transduces HER2^{+} cells in a target antigen dependent manner

The HER2-AAV used in this study harbors a coding sequence for a fusion protein directed against murine PD-1 (HER2-AAV[aPD1]) (depicted in Figure 3a-c). The human Fc part used previously[28] was replaced by the corresponding murine sequence (Figure 3c). HER2-AAV[IgG-Fc] encoding only the murine Fc part of aPD-1 served as a control (Figure 3a, right). Detection of the recombinant aPD-1 was facilitated by addition of a HA-tag (Figure 3b).

Upon transduction of target cells with HER2-AAV[aPD−1], we detected mRNA of the aPD-1 transgene only in HER2^{+} cells (Figure 3d). We also quantified secreted aPD-1 protein in the supernatant of transduced cells via ELISA, showing that only HER2^{+} target cells which were incubated with HER2-
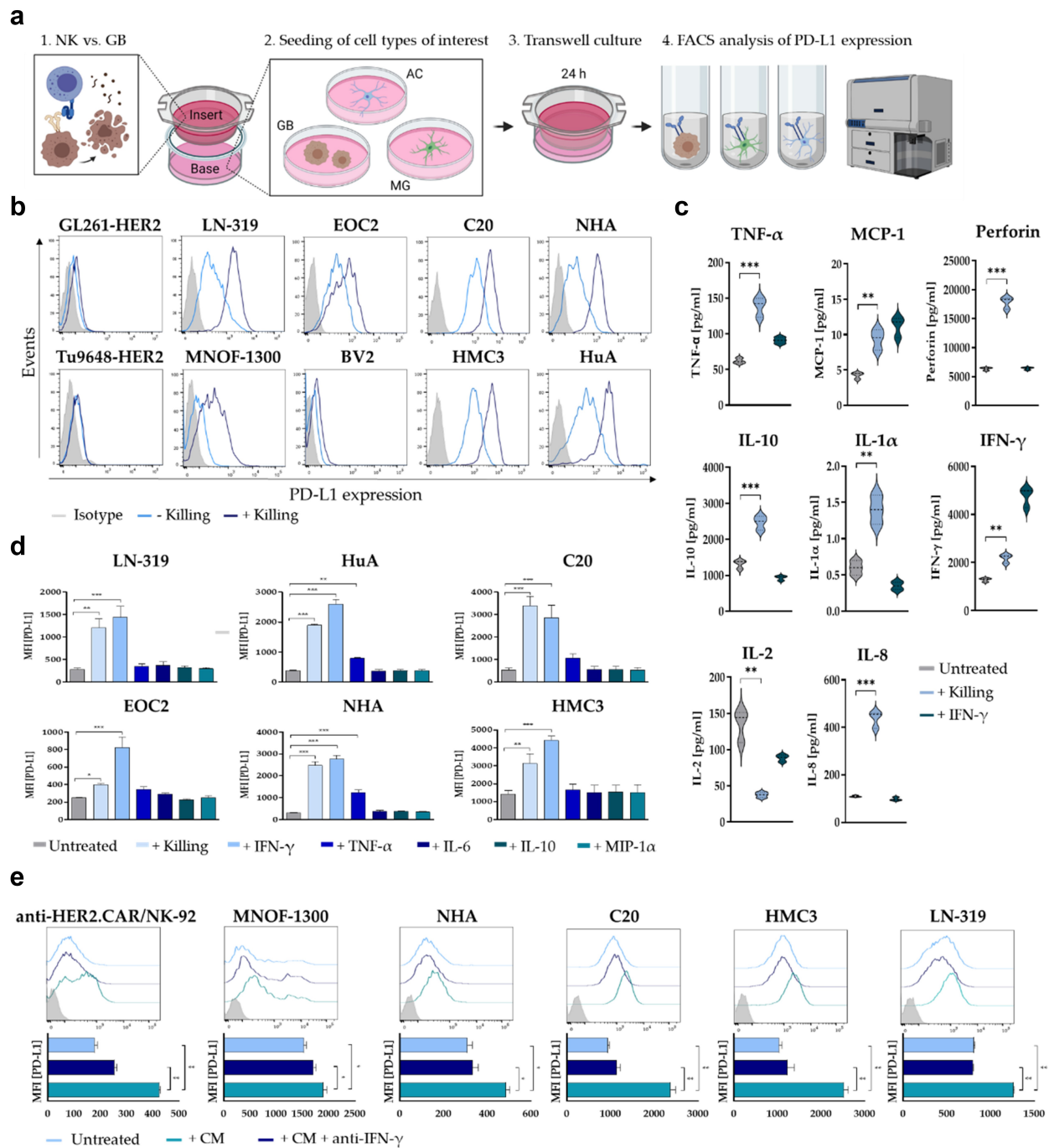
Figure 2. PD-L1 regulation in response to anti-HER2.CAR/NK-92 cell-mediated tumor cell lysis. (**a**) Schematic representation of the PD-L1 transwell assay design. Soluble factors secreted from stimulated anti-HER2.CAR/NK-92 cells in the insert influence cells of interest in the base (GB: glioblastoma cells, AC: astrocytes, MG: microglia). (**b**) PD-L1 regulation in response to a transwell cytotoxicity assay was analysed on murine (GL261, Tu9648) and human (LN-319, MNOF-1300) glioma cell lines as well as on murine (EOC2, BV2) or human (C20, HMC3) microglia and human astrocyte (NHA, HuA) cell lines via flow cytometry. Cells of interest were seeded in wells (base) of a 24-well plate, while a cytotoxicity assay was performed in the insert (E/T ratio 1:1, murine cells of interest: anti-HER2.CAR/NK-92 vs. GL261-HER2, human cells of interest: anti-HER2.CAR/NK-92 vs. LN-319). After 24 h, PD-L1 expression of cells in the base was determined via flow cytometry. (**c**) Analysis of cytokine release by stimulated anti-HER2.CAR/NK-92 cells. Concentrations of IFN-γ, TNF-α, MCP-1, IL-1α, IL-2, IL-8, IL-10 and perforin were measured in cell culture supernatants using a Luminex multiplex bead assay. hIFN-γ [100ng/ml] served as positive control for cell stimulation. Mean values ± SD are shown; n=3. **p < 0.01, ***p < 0.001. (**d**) PD-L1 regulation in various cell types in response to stimulation with species-compatible (human/murine) recombinant cytokines was analysed via flow cytometry. Cells were incubated with recombinant cytokines for 24 h at a concentration of 100 ng/ml. Mean values ± SD are shown; n=3, *p < 0.05, **p < 0.01, ***p < 0.001. (**e**) PD-L1 expression was assessed via flow cytometry upon cultivation in conditioned medium from a cytotoxicity assay (E/T ratio 1:1, anti-HER2.CAR/NK-92 vs. LN-319) either in the absence or presence of anti-human IFN-γ antibody for 24 h. Mean values ± SD are shown; n=3. *p < 0.05, **p < 0.01.

AAV^{aPD-1} produced the immunoadhesin (Figure 3e). Moreover, aPD-1 levels correlated well with the expression level of human HER2 on the target cells (Figure 1a and 3f, Figure S4c). Furthermore, aPD-1 levels were higher in supernatant of LN-319-HER2 cells modified to further over-express HER2 when compared to parental HER$^+$ LN-319 cells (Figure 3d-f). Notably, also HER2$^+$ human primary glioma cells expressed aPD-1 upon exposure to HER2-AAV^{aPD-1}
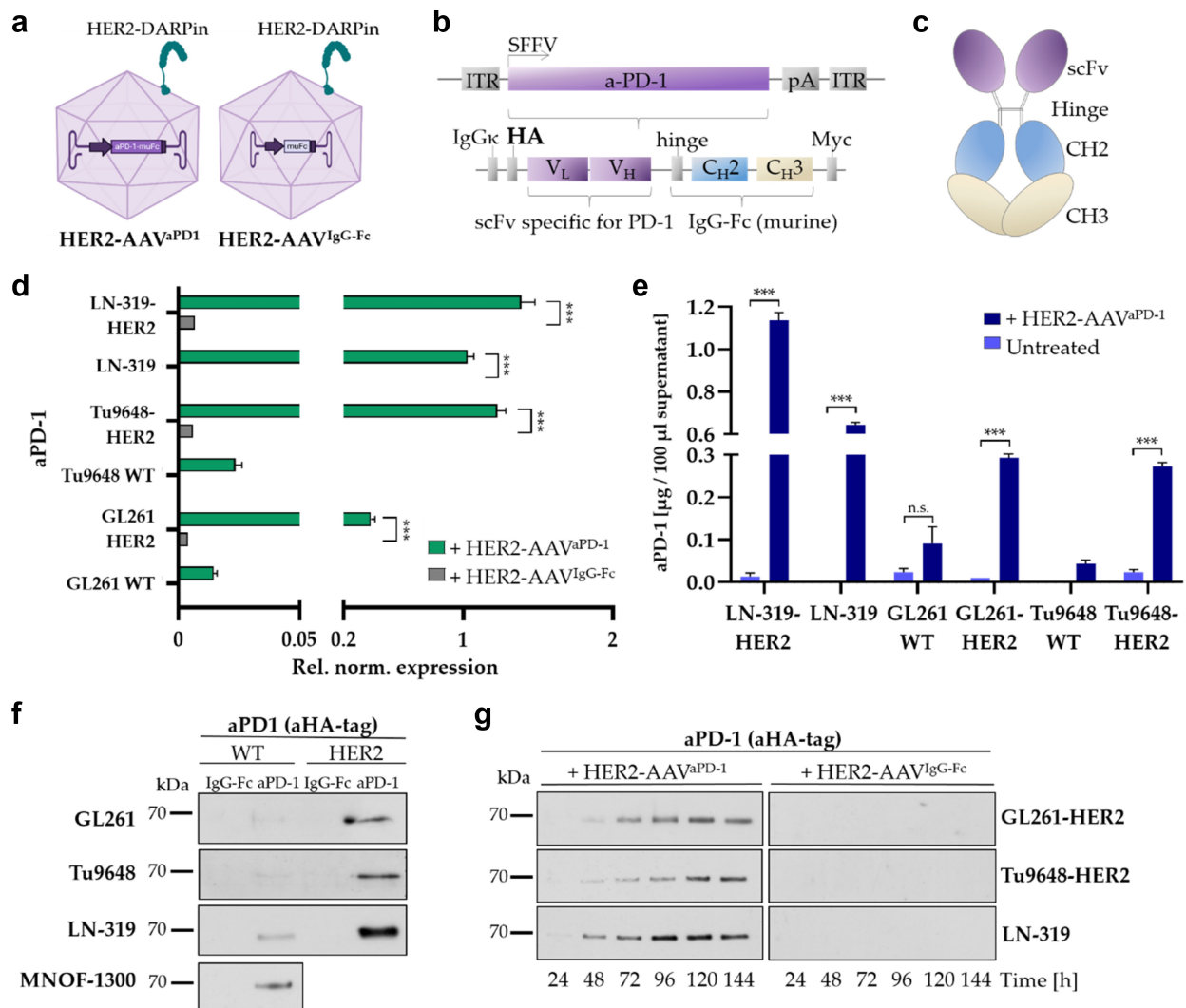
Figure 3. ICI gene delivery by HER2-AAV. (**a**) HER2-AAVaPD-1 encodes an immunoadhesin directed against murine PD-1 (left). As a control, HER2-AAV$_{IgG-Fc}$ encoding the Fc part was used (right). (**b**) Schematic representation of the transfer vector encoding HA-tagged murine aPD-1. (**c**) Scheme of the immunoadhesin directed against murine PD-1. (**d**) Quantification of transgene expression on the mRNA level as determined by qPCR. RNA wasisolated four days post transduction; SDHA and 18s were used as housekeeping genes for reference. (Rel. norm. values ± SD are shown; n=3. ***p < 0.001). (**e**) Supernatants of *in vitro* transduced glioma cells were analyzed by ELISA using an HA-specific antibody. Non-transduced target cells and murine wildtype (WT) cells not expressing the target antigen were used as controls. Mean values ± SD are shown; n=3. ***p < 0.001. (**f**) *in vitro* gene delivery by HER2-AAV. Four days post incubation with HER2-AAV (4.5x105 genome copies/cell), cell culture supernatants were collected and aPD-1 expression was analyzed via Western blot using an HA-specific antibody. (**g**) aPD-1 transgene expression over time in GL261-HER2 (top), Tu9648-HER2 (middle) and LN-319 (bottom) cells monitored by Western blot analysis using an HA-specific antibody.

(Figure 3f and Figure S4a). Levels of aPD-1 accumulated over time and persisted for up to 1 week without signs of degradation in the cell culture supernatant as well as in cell lysates (Figure 3g and Figure S4b).

AAV-encoded aPD-1 binds its target and blocks the PD-1/PD-L1 interaction

To functionally characterize HER2-AAV encoded aPD-1, we investigated its capacity to recognize PD-1 and block its activity. Specific target binding was assessed via a binding assay employing HT1080 cells overexpressing PD-1 as depicted in Figure 4a. After transduction of murine and human glioma cells, specific binding of the aPD-1 immunoadhesin contained in the supernatant to PD-1 on HT1080-PD1 cells was found (Figure 4b-c). Similar results were obtained with PD-1-expressing freshly isolated

murine splenocytes (Figure 4d). To further confirm the functionality of the aPD-1 immunoadhesin, we also performed a PD-1/PD-L1 blockade bioassay using T cells which express an NFAT-regulated reporter gene (Figure 4e). Supernatant containing aPD-1-immunoadhesin was able to interrupt the PD-1/PD-L1 axis and to reestablish TCR activation in these cells, thus demonstrating the ability of HER2-AAV encoded aPD-1 to reactivate T cells upon PD-1 blockade *in vitro* (Figure 4f).

HER2-AAV transduction does not decrease HER2 expression or interfere with anti-HER2.CAR/NK-92 cell cytotoxicity

In order for target cells to produce and secrete the immunoadhesin, the viability of transduced tumor cells should not be excessively impaired. Target cell proliferation did not
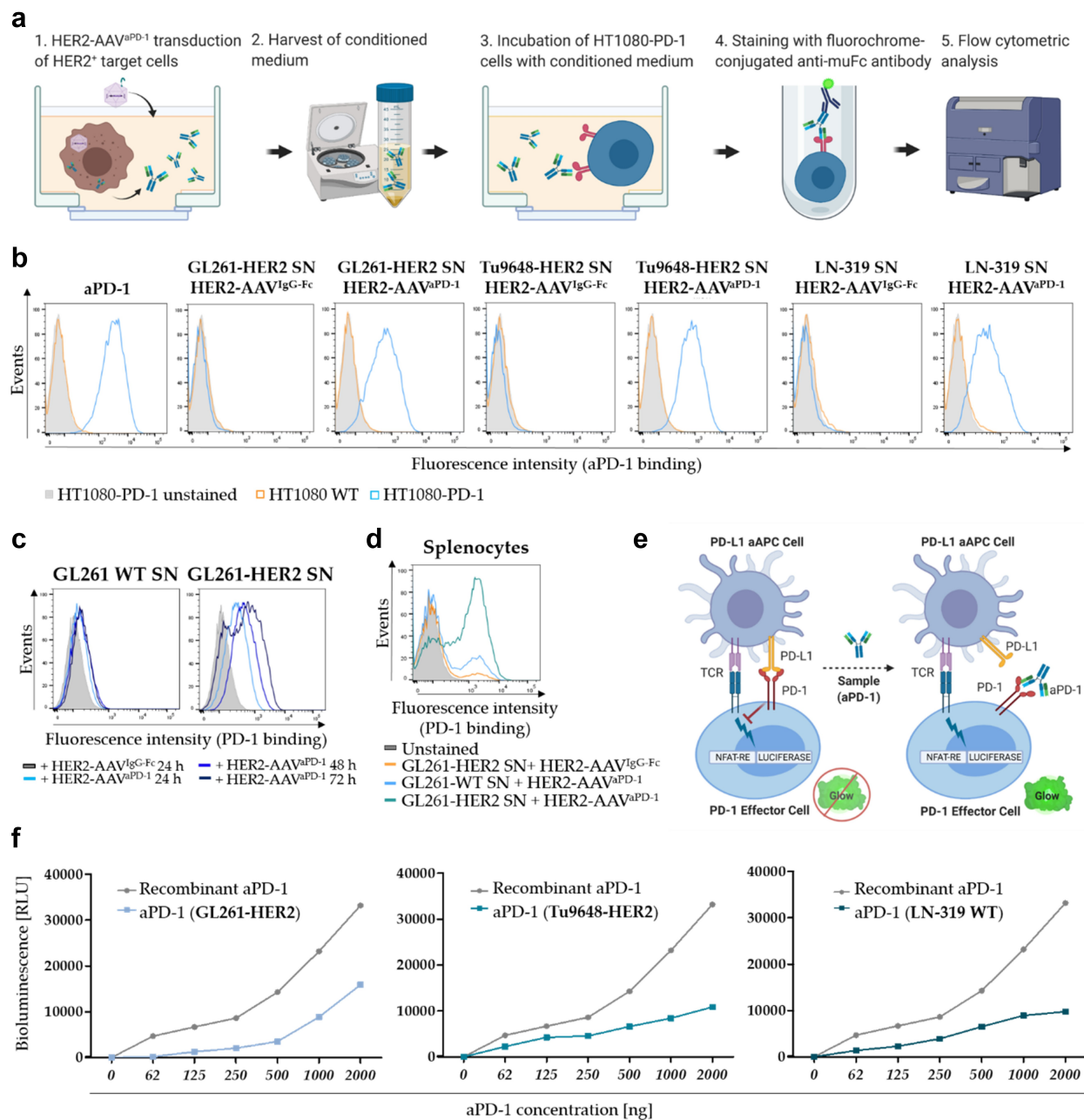
Figure 4. Functionality of HER2-AAV encoded aPD-1. (**a**) Schematic representation of the aPD-1 binding assay. Binding of secreted aPD-1 to PD-1 expressing HT1080-PD1 cells was detected by flow cytometry via a murine IgGFc-specific antibody. (**b**) Specific binding of HER2-AAV-encoded aPD-1 to HT1080-PD1 (blue profiles) and PD-1 negative HT1080 WT cells (gray profiles).Supernatants (SN) from glioma cells that were transduced with HER2-AAV$_{aPD-1}$ or the control HER2-AAV$_{IgG-Fc}$ were tested; recombinant aPD-1 served as positive control. (**c**) Analysis of aPD-1 target binding in a time dependent manner. Cell culture supernatant of transduced GL261 cells (WT and HER2+) was harvested at different time points post transduction and was used for an aPD-1 binding assay. (**d**) Specific target antigen recognition of HER2-AAV encoded aPD-1 on PD-1 expressing splenocytes. Freshly isolated murine splenocytes were stimulated with CD3/CD28 Dynabeads for 48 h in order to upregulate PD-1 expression, before SN of transduced GL261-HER2 cells was added. (**e**) Schematic representation of the PD-1/PD-L1 blockade bioassay. PD-L1-expressing aAPC/CHO-K1 target cells harbor an engineered cell surface protein mediating antigen-independent activation of T cells. The cells were incubated with PD-1 expressing effector T cells carrying a luciferase reporter driven by an NFAT response element. aPD-1 in the cell culture supernatant disrupts the PD-1/PD-L1 interaction between aAPC/CHO-K1 target cells and T cells. This allows activation of T-cell receptors, resulting in luciferase expression via NFAT activation. (**f**) After addition of aPD-1-containing cell culture supernatant, TCR activation was measured by assessing NFAT-dependent induction of luciferase expression. Bioluminescence is represented in relative light units (RLU). Recombinant aPD-1 served as positive control.

significantly decrease upon transduction (Figure S5a); however, a slight, yet significant increase in cell death was observed in response to HER2-AAV^{aPD-1} transduction (Figure 5a). Since HER2 was chosen as a target antigen for both transduction by AAVs and tumor cell killing by anti-HER2.CAR/NK-92 cells, we investigated whether transduction of glioma cells with the AAV vector might lead to downregulation of HER2.

Thereby, we did not observe a change in HER2 expression in response to transduction (Figure 5b). When combining anti-HER2.CAR/NK-92 cells with HER2-AAV, it is essential that HER2-AAV transduction of tumor cells does not interfere with anti-HER2.CAR/NK-92 cell-mediated killing or reduce anti-HER2.CAR/NK-92 cell viability. In a comparative cytotoxicity assay, no difference in the killing efficiency of anti-HER2.CAR/
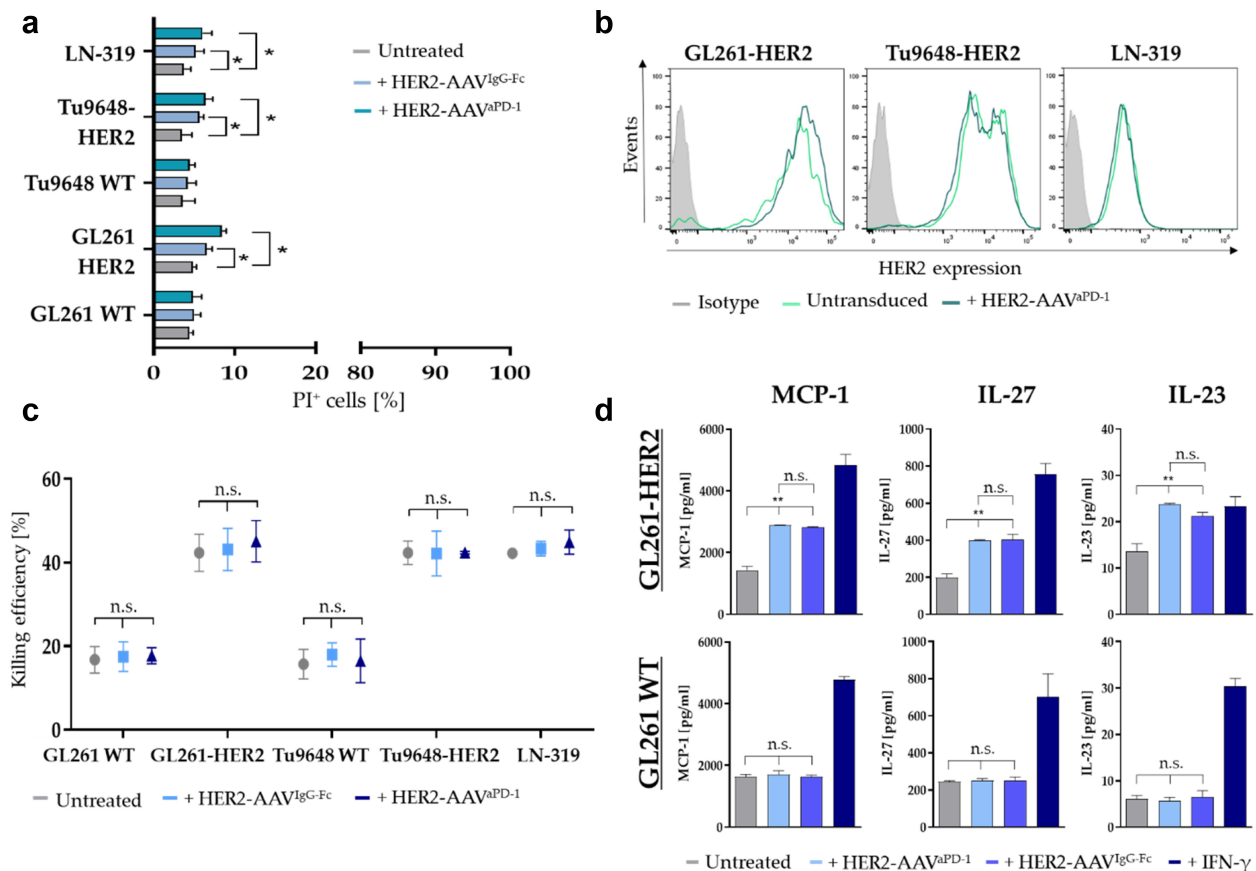
Figure 5. Effect of HER2-AAV on target cells and killing capacity of anti-HER2.CAR/NK-92 cells. (**a**) Viability of glioma cells 24 h post transduction with HER2-AAV_{IgG-Fc} (light blue) or HER2-AAV_{aPD-1} (petrol) as determined by propidium iodide (PI) FACS. Mean values ± SD are shown; n=3. *p < 0.05. (**b**) HER2 expression in response to HER2-AAV was determined 24 h after transduction via flow cytometry. (**c**) Killing efficiency of anti-HER2.CAR/NK-92 cells towards murine glioma cells was assessed 72 h post transduction with a cytotoxicity assay (2 h co-culture at an effector to target ratio of 5:1); Mean values ± SD are shown; n=3. (**d**) Levels of various inflammatory cytokines produced by murine GL261-HER2 (top) or WT (bottom) cells in response to transduction with HER2-AAV_{aPD-1} as compared to transduction with HER2-AAV_{IgG-Fc} determined with a bead-based immunoassay. As a positive control, cells were stimulated with recombinant murine IFN-γ [100ng/ml]. Mean values ± SD are shown; n=3. *p < 0.05, **p < 0.01.

NK-92 against transduced or untransduced glioma cells was found (Figure 5c).

The release of inflammatory cytokines by tumor cells can be of substantial importance for their effects on neighboring immune cells. Therefore, we analyzed cytokine secretion of both, GL261-HER2 and GL261 WT cells in response to HER2-AAV transduction. To rule out the possibility that transduction of murine glioma cells with the HER2 antigen affected cytokine secretion, we also assessed basal cytokine levels of GL261-HER2 cells in comparison to GL261 WT cells. We did not find significant changes in the levels of IFN-γ, CXCL1, TNF-α, MCP-1, IL-12p70, IL-27, IL-1β, GM-CSF, IL-10, IFN-β and IFN-α (Figure S6a), with the exception of IL-23, where we observed a significantly increased secretion in GL261-HER2 cells. Upon transduction with HER2-AAVs, we found increased secretion of cytokines such as MCP-1, IL-23 and IL-27 only in GL261-HER2 target cells, with a similar effect of HER2-AAV^{aPD-1} and HER2-AAV^{IgG-Fc} transduction (Figure 5d, top). In contrast, GL261 WT cells lacking the antigen retained baseline levels (Figure 5d, bottom). Levels of IFN-γ, CXCL-1, TNF-α, IL-12p70, IL-1β, GM-CSF, IL-10, IFN-β and IFN-α remained unchanged (Figure S6b).

HER2-AAV targets tumor tissue upon intratumoral and intravenous injection *in vivo*

In a comparative transduction kinetics study *in vivo*, we investigated tumor cell transduction by HER2-AAV and production of the HA-tagged immunoadhesin following intravenous (i.v.) or intratumoral (i.t.) injections of the vector in subcutaneous or orthotopic intracranial tumors (Figure 6a). Continuous expression of the human HER2 target antigen by the glioblastoma cells 8 weeks post initial subcutaneous tumor cell injection was confirmed (Figure S7a). Interestingly, the analysis of explanted tumors also revealed upregulation of PD-L1 by the tumor cells *in vivo*, further emphasizing the importance of checkpoint inhibition for anti-tumor immune responses (Figure S7b). Nevertheless, this upregulation of PD-L1 expression was similar for untreated tumors and tumors treated with anti-HER2.CAR/NK-92 (Figure S7c).

To verify transduction efficacy and to investigate kinetics of aPD-1 production in human glioma cells *in vivo* without potential immune responses against the vector, Crl:NU(NCr)-Foxn1^{nu} mice were subcutaneously injected with LN-319 cells as a xenograft model. aPD-1 was expressed in all injected tumors, irrespective of the AAV administration route
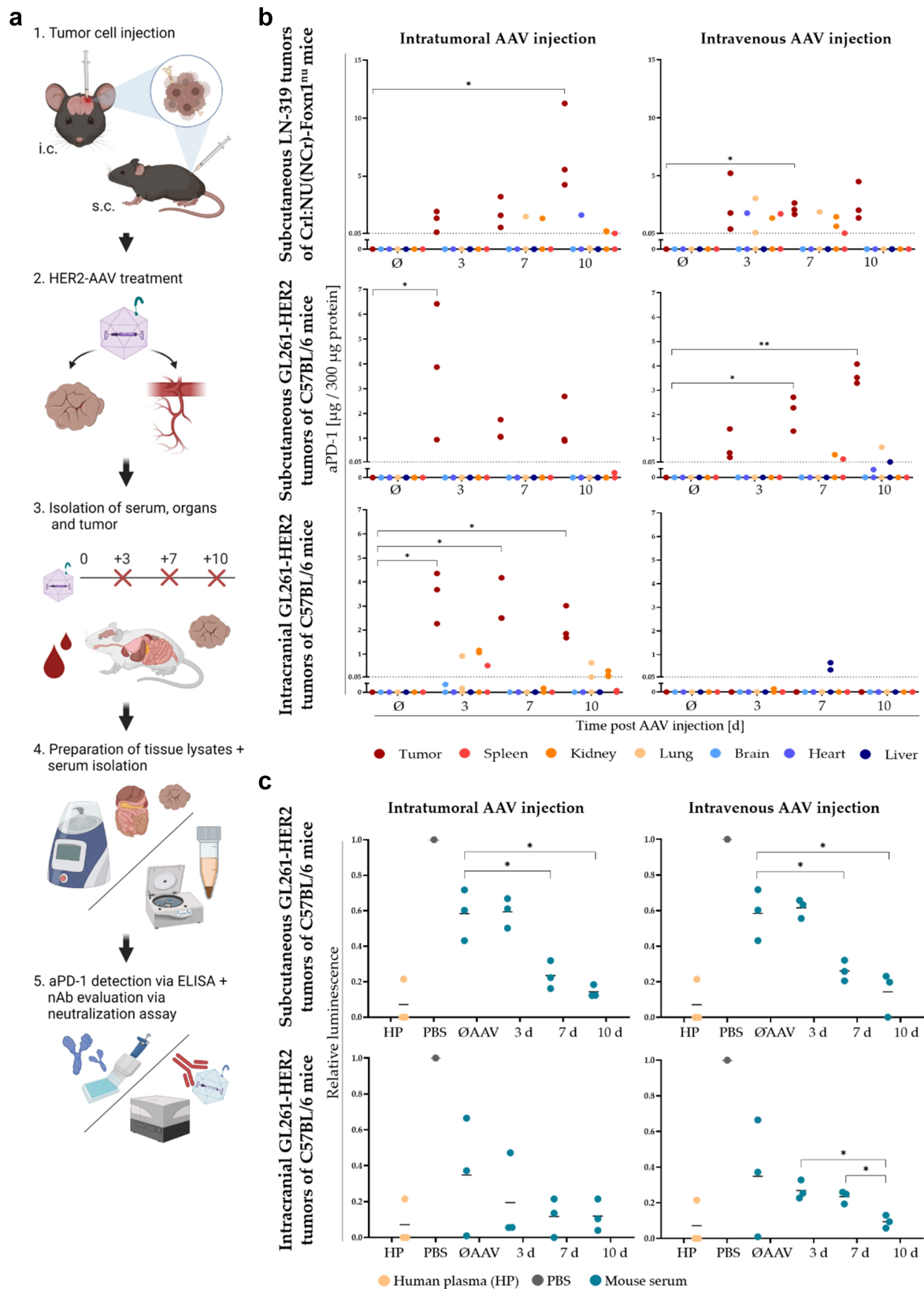
Figure 6. Distribution kinetics of HER2-AAV-encoded aPD-1 in vivo and generation of neutralizing antibodies. (**a**) Workflow of the kinetics study analyzing secreted aPD-1 and neutralizing antibodies (nAbs). HER2-AAV$_{aPD1}$ vector was injected either intravenously or intratumorally into subcutaneous or intracranial GL261-HER2 tumors in syngeneic C57Bl/6 mice. Serum and tissues were obtained 3, 7 and 10 days post HER2-AAV injection, and aPD-1 concentrations as well as the presence of nAbs were evaluated by ELISA and neutralization assays, respectively. (**b**) aPD-1 concentration in tumor tissue and organs in the subcutaneous xenograft (top), the subcutaneous syngeneic (middle) and the orthotopic intracranial (bottom) mouse glioblastoma model after intratumoral (left) and intravenous (right) AAV administration determined by ELISA. Organ and tumor lysates of untreated mice served as negative controls. The dotted line represents the detection limit. Negative values were set to 0 for illustration. n=3. (**c**) The generation of nAbs in syngeneic subcutaneous (top) and orthotopic intracranial (bottom) mouse models was evaluated using a luminescence-based neutralization assay. Relative luminescence in comparison to transduction control in the absence of serum is indicated (PBS). Pooled human plasma (HP) was used as a positivecontrol, since about 70% of humans are seropositive for antibodies reactive with AAV2. Sera of untreated mice (ØAAV) or mice sacrificed 3, 7 or 10 days post HER2-AAV injection were analyzed (individual values are shown as dots, black bars represent mean values, n=3. *p < 0.05, **p < 0.01).

(Figure 6b, top). Thereby, aPD-1 concentrations increased in a time-dependent manner after HER2-AAV administration, reaching a maximum at day 10 after intratumoral injection (mean value of 7.2 µg aPD-1 per 300 µg protein, Figure 6b, top left).

aPD-1 was detected in all tumor samples post intravenous or intratumoral AAV administration in the syngeneic subcutaneous GL261-HER2 glioblastoma model in immunocompetent mice, similar to the LN-319 xenograft model in immunodeficient animals (Figure 6b, middle). In the cohort of intratumorally treated mice, maximum aPD-1 amounts were observed at day 3 post transduction with a mean value of 3.7 µg aPD-1 per 300 µg protein (Figure 6b, middle left). Still, this concentration was 2-fold lower than the mean maximum reached in tumors of intratumorally injected immunodeficient Crl:NU(NCr)-Foxn1^{nu} mice. Overall aPD-1 concentrations were only slightly lower than in tumors of immunodeficient mice (mean values of 6.4 µg (intratumorally treated C57BL/6 mice) vs. 7.3 µg (intratumorally treated Crl:NU(NCr)-Foxn1^{nu} mice) per 300 µg protein, respectively). Besides tumors, measurable amounts of aPD-1 were only found in one kidney (0.18 µg aPD-1 per 300 µg protein) post intratumoral HER2-AAV injection (Figure 6b, middle left). In mice that had received intravenous HER2-AAV injections, a steady and significant increase in aPD-1 concentrations in tumor tissue over time was observed, ranging from mean values of 0.7 µg on day 3 to 2.1 µg on day 7, and 3.6 µg aPD-1 per 300 µg protein on day 10 (Figure 6b, middle right). In this case, aPD-1 was detected in spleen, kidney, liver and lung; however, in these tissues aPD-1 concentrations only ranged from 0.05 µg (C57BL/6 mice) to 0.66 µg (Crl:NU(NCr)-Foxn1^{nu} mice) per 300 µg protein. In general, the amount of aPD-1 in peripheral organs was lower in this model as compared to the xenograft model (mean value of 0.35 µg (C57BL/6 mice) vs. 1.6 µg (Crl:NU(NCr)-Foxn1^{nu} mice) per 300 µg protein, respectively). Notably, the transduction activity of HER2-AAV was inhibited by sera of untreated mice (Figure 6c, top). Sera from injected animals reduced the gene transfer activity of HER2-AAV further, with the strongest inhibitory effect observed with sera obtained 7 and 10 days post intratumoral HER2-AAV injection (Figure 6c). Similar results were obtained after intravenous administration of the vector, indicating generation of nAbs regardless whether HER2-AAVs was injected locally or systemically.

Repeated injections (on day 0 and day 3) of HER2-AAV did not lead to higher aPD-1 concentrations in this model, irrespective of the administration route (data not shown). However, the level of nAbs was significantly increased in response to repeated HER2-AAV injections in the sera of animals bearing subcutaneous GL261-HER2 tumors (Figure S8b, left+middle). Importantly, *in vivo* secreted aPD-1 was functional, as confirmed by the analysis of aPD-1-containing tumor interstitial fluid (TIF), which revealed aPD-1 binding to PD-1 *in vitro* (Figure S7c).

Similarly, in orthotopic GL261-HER2 tumors of immunocompetent C57BL/6 mice intratumorally injected with HER2-AAV^{aPD-1}, aPD-1 was detectable in all tumors, ranging from 1.7 to 4.4 µg aPD-1 per 300 µg total protein (Figure 6b, bottom). The maximum concentration was observed 3 days post

HER2-AAV injection with a mean value of 3.9 µg aPD-1 in 300 µg total protein. Small amounts of aPD-1 were also found in lung, kidney and spleen. The aPD-1 levels in tumors slightly decreased over time. The inhibitory activity of mouse sera on transduction increased over time, suggesting the formation of nAbs (Figure 6c, bottom). The same time-dependent effect was observed after intravenous AAV administration. Notably, in the orthotopic tumor model no aPD-1 was detected in brain tumors after intravenous HER2-AAV administration (Figure 6b, bottom right).

To assess the anti-tumor effect of HER2-AAV^{aPD1}, anti-HER2.CAR/NK-92 cells or the combination of both, we employed a subcutaneous GL261-HER2 immunocompetent mouse model. Treatment was initiated when tumors reached a size of 40 mm^3 (Figure 7a). Mice which received the combination therapy with anti-HER2.CAR/NK-92 cells and HER2-AAV^{aPD-1} showed slower tumor growth and significantly increased symptom-free survival as compared to the control groups, irrespective of the HER2-AAV vector administration route (i.v. vs. i.t., Figure 7b, Figure S8d). In some of the mice the combination therapy achieved complete tumor rejection (anti-HER2.CAR/NK-92 + HER2-AAV^{aPD-1} i.t.: 3 of 5 animals; anti-HER2.CAR/NK-92 + HER2-AAV^{aPD-1} i.v.: 2 of 5 animals), indicating the induction of a potent anti-tumor immune effect in response to combination therapy. In larger, more advanced GL261-HER2 tumors, where treatment was initiated when tumors exceeded a volume of 80 mm^3, a similar yet less pronounced therapy effect of local anti-HER2.CAR/NK-92 + HER2-AAV^{aPD-1} therapy was observed (Figure S9). To further explore this approach in a completely unrelated glioblastoma model, we also investigated the effects of the treatment in mice carrying Tu2449 tumors. Tu2449 cells were originally derived from a tumor that arose spontaneously in a glial fibrillary acid protein (GFAP)-v-*src* transgenic mouse.[39] In this model, we observed a deceleration of tumor growth upon combined local anti-HER2.CAR/NK-92 + HER2-AAV^{aPD-1} treatment (Figure S10). We did not observe weight loss or other signs indicating treatment-related toxicities in any of the treatment groups or glioblastoma models applied.

Discussion

Immunotherapy as an emerging field in cancer therapy aims toward the induction of an immune response directed against tumor antigens, and so elicit anti-tumor effects. Since GB is characterized by low immunogenicity of tumor cells combined with prevalent immunosuppression within the TME, release of tumor antigens from lysed tumor cells upon anti-HER2.CAR/NK-92 cell therapy in combination with local intratumoral checkpoint inhibition through aPD-1-encoding HER2-AAV may represent a promising novel treatment approach for the clinical management of GB.

Here, we evaluated the two components of the combination therapy approach regarding their applicability, their effects on target and bystander immune cells as well as their impact on *in vivo* tumor control.

The potent cytolytic effect of anti-HER2.CAR/NK-92 cells against HER2$^+$ cells *in vitro* has been demonstrated before and was confirmed by our studies with several
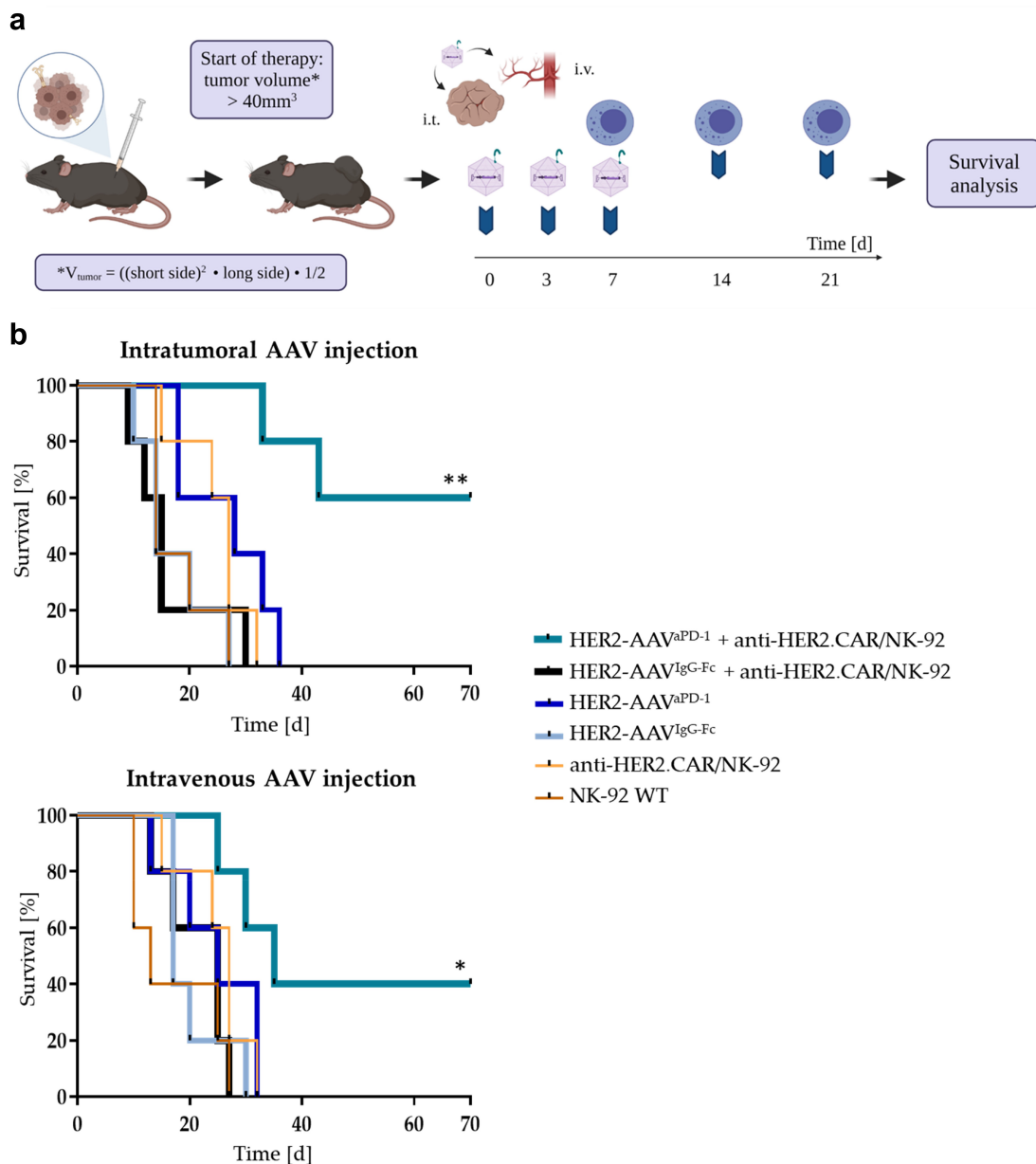
Figure 7. Survival benefit upon combination therapy in mice bearing subcutaneous HER2+ tumors. (**a**) Therapy scheme for subcutaneous GL261-HER2 tumors in immunocompetent C57BL/6 mice. Mice received HER2-AAV injections either intratumorally or intravenously (1×10^{11} genome copies (gc)/injection) at day 0, 3 and 7. At day 7, 14 and 21, intratumoral injections of anti-HER2. CAR/NK-92 cells (1×10^{7} cells/injection) were administered. (**b**) Symptom-free survival rates of different mouse cohorts after single or combined treatment with HER2-AAV$_{aPD-1}$ orHER2-AAV$_{IgG-Fc}$ (intratumoral (i.t., top) and intravenous (i.v., bottom) administration) and anti-HER2. CAR/NK-92 cells (intratumoral administration) (n= 5 per group, *p < 0.05, **p < 0.01 Log-rank Mantel-Cox test).

murine and human glioma cell lines, including primary human glioma cells[5] (Figure 1b+c, Figure S1f). *In vivo*, the release of tumor antigens following tumor cell lysis by adoptively transferred anti-HER2.CAR/NK-92 cells could support subsequent anti-tumor immune responses via the activation of endogenous antigen presenting cells (APCs) and T cells.[40] We showed in *in vitro* co-culture models that surrounding cells reflecting cell types present in the TME reacted to target-activated anti-HER2.CAR/NK-92 cells, resulting in tumor cell lysis and the secretion of various inflammatory cytokines (Figure 1e). Especially in immune cells like microglia (MG), levels of IL-6 and IL-8 were significantly increased in response to tumor cell lysis. IL-6 is known to be secreted by macrophages and is of

importance in tumor control as it is able to antagonize the effects of regulatory T cells (Tregs).[41,42]

Furthermore, we found upregulation of the checkpoint protein PD-L1 in response to anti-HER2.CAR/NK-92 cell therapy, which may contribute to sustained immunosuppression within the TME and inhibition of anti-tumor responses.[23] Increased PD-L1 expression was not only seen on glioblastoma cells, but also on immune cells such as MG and astrocytes (Figure 2b and Figure S3a) which are part of the TME *in vivo*, indicating a possible further immunoregulatory effect after administration of anti-HER2.CAR/NK-92 cells. NK cells in general have been reported to produce Th1-type cytokines including IL-1β, IL-12, TNF-α, and IFN-γ upon activation by tumor cells.[43,44] While our data are consistent with the literature (Figure 2c,[19]),

we moreover found significantly increased levels of MCP-1 (two-fold), perforin (three-fold) and IL-1α (two-fold). Such pro-inflammatory factors can contribute to the activation of effector lymphocytes and myeloid cells.[45–47] In our setting, PD-L1 upregulation on surrounding cells in response to anti-HER2.CAR/NK-92 cell activation was mainly caused by IFN-γ secreted by the anti-HER2.CAR/NK-92 cells (Figure 2d+e), which was reported to be the major driver of PD-L1 expression in cells of the TME.[48–50] Our findings are consistent with a report from another group describing IFN-γ induced PD-L1 expression on GL261 glioma cells, macrophages and MG.[51] Upregulation of checkpoint molecules in glioma has previously been reported.[52] Likewise, we found increased PD-L1 expression on murine tumor cells in our GL261-HER2 model in vivo (Figure S7b). Since this effect might be intensified upon anti-HER2.CAR/NK-92 cell therapy further promoting the suppression of endogenous antitumor immune reactions, the combination of anti-HER2.CAR/NK-92 cells with an ICI like aPD-1 appears highly warranted. Thereby, administration of an aPD-1 encoding HER2-AAV that selectively targets tumor cells and mediates local aPD-1 expression may disrupt immunosuppression by blocking the PD-1/PD-L1 axis.

Accordingly, we studied tumor-cell specific gene transfer of aPD-1 via targeted HER2-AAV as an alternative delivery strategy for ICIs, since systemic application of monoclonal ICI antibodies typically results in low tissue concentrations, with a maximum of 5–10% of the administered amount reaching the target tissue.[53] Selective transfer of an ICI-encoding gene by engineered HER2-AAV vectors has previously been investigated in a murine renal cell carcinoma model.[28] Our data demonstrate efficient transduction of HER2-expressing glioma cells of murine and human origin by HER2-AAV^{aPD-1}, and high expression of aPD-1 on the mRNA and protein level (Figure 3d-f). After target cell transduction, the AAV vector genome persists in the host cell as an episome, and transgene expression is maintained for the lifetime of the cell.[54,55] In our experiments, we found constant aPD-1 protein levels in transduced cells 10 days after initial transduction, indicating stable gene expression upon vector entrance (Figure S4b). Of note, gene expression has been reported to be maintained for years in post-mitotic cells such as muscle cells after a single AAV injection.[56] Hence, permanent ICI production could bear the risk of potentially fatal immune-related adverse events (irAEs).[57] Nevertheless, ensuing immune reactivity against the aPD-1 producing tumor cells and tumor cell lysis will likely decrease ICI release, with mitotic activity of potentially surviving tumor cells resulting in a loss of the transgene over time.

We confirmed functionality of HER2-AAV encoded aPD-1 in vitro and in vivo, indicating correct folding and dimerization of the protein as well as disruption of the PD-1/PD-L1 axis and subsequent re-activation of T-cell activity (Figure 4b-f, Figure S7d). Furthermore, in contrast to anti-HER2.CAR/NK-92 cell therapy, HER2-AAV transduction did not induce upregulation of PD-L1 expression on tumor cells (Figure S5b). Since anti-HER2.CAR/NK-92 cells do not express HER2, they do not serve as targets for HER2-AAV (Figure S5c and d). There was also no direct effect of HER2-AAV transduction on the sensitivity of tumor cells to anti-HER2.CAR/NK-92 cell cytotoxicity (Figure 5c). Even though HER2 is internalized via receptor

mediated endocytosis following ligand binding,[58] the receptor is typically recycled and brought back to the cell membrane rather than degraded in the lysosome.[59] The increased secretion of the cytokines MCP-1, IL-23 and IL-26 by GL261-HER2 cells was induced by HER2-AAV rather than aPD-1 production, as it did not significantly differ between GL261-HER2 cells transduced with HER2-AAV^{aPD-1} and HER2-AAV^{IgG-Fc} (Figure 5d).

Since knowledge about the in vivo secretion of HER2-AAV encoded aPD-1 is crucial for the implementation of a combination therapy with anti-HER2.CAR/NK-92 cells, we evaluated aPD-1 biodistribution kinetics in immunodeficient and immunocompetent mouse models. In both cases, high transduction rates were achieved, resulting in high levels of aPD-1 in subcutaneous tumors as compared to peripheral organs. Nevertheless, it remains to be determined which intratumoral aPD-1 levels need to be reached for therapeutic activity. Our data suggest that intratumoral and intravenous administration routes are equally efficient for subcutaneous tumors (Figure 6b). In orthotopic intracranial tumors, aPD-1 was only found upon intratumoral vector administration, suggesting that HER2-AAV is not able to cross the blood-brain barrier (BBB) and reach the tumor from the periphery (Figure 6b). Nevertheless, after direct local injection into brain tumors, HER2-AAV may still enter the bloodstream and potentially transduce cells in other organs. Also, aPD-1 protein locally produced by tumor cells may be transported to the periphery via the vasculature. Nevertheless, our data suggest that vector-encoded aPD-1 mainly remains within the tumor, with only a low level of spillage of either HER2-AAV or secreted aPD-1 to peripheral organs. While minimal off-target effects following HER2-AAV administration have been reported before,[28] aPD-1 levels in organs were ~20 times lower than in tumor tissue, indicating a high transduction selectivity and specificity. This should also reduce the risk of liver toxicity observed after intravenous AAV2 injections.[31,60] Local expression of aPD-1 in the TME of brain tumors did not result in an excessive increase in serum concentrations of inflammatory cytokines. There was, however, a trend toward an increase in IFN-γ, TNF-α, MCP-1 and IL-10 10 days after vector administration, and significantly increased levels of IL-23 were found (Figure S8c). This effect might be caused by an immune reaction directed against the secreted immunoadhesin, or even side effect of an anti-tumor response due to aPD-1-induced re-activation of the immune system. A major challenge in AAV mediated gene therapy is the generation of neutralizing antibodies against the vector capsid. Natural exposure to wild-type AAV triggers humoral immunity early in life, and antibodies directed against serotype 2 have been shown to be most prevalent in humans, with up to 70% seropositivity.[61,62] It has also been reported that sera of laboratory animals can contain preexisting antibodies against AAV serotypes AAV1, AAV2, AAV6 and AAV9.[63] Notably, in our experiments transduction efficacy of HER2-AAV was inhibited by sera of untreated mice, confirming the preexistence of nAbs against AAV2 in our cohort of animals. In mice injected with HER2-AAV, nAb titers increased over time after a single injection (Figure 6c), which might explain why repeated injections of the vector did not result in higher aPD-1 concentrations. In fact, repeated

injections led to increased nAb titers, regardless of the administration route (Figure S8b). To avoid recognition by nAbs, further modifications aiming to shield neutralizing epitopes on the AAV capsid surface have previously been evaluated. For instance, crosslinking synthetic polymers such as polyethylene glycol to the capsid surface has been performed by several groups, and indeed resulted in reduced neutralization activity.[64] Furthermore, due to its intrinsic tropism, AAV9 may be preferred for the transduction of brain tissue following intravenous administration, and the prevalence of nAbs directed against this serotype is lower in humans.[65,66]

Nevertheless, intratumoral as well as intravenous injection of HER2-AAV^{aPD-1} resulted in a significant therapeutic benefit without treatment-related side effects in a subcutaneous GL261-HER2 glioblastoma model in immunocompetent mice, even leading to complete tumor rejection in some of the animals (Figure 7b, Figure S8d). Similar to other immunotherapeutic approaches, we observed a response to the combination therapy only in some of the animals. The extent of the treatment effect depended on tumor size, and was less pronounced in larger, more advanced tumors (Figure S9). We also observed a reduced tumor growth after combined local anti-HER2.CAR/NK-92 and HER2-AAV^{aPD-1} treatment in the subcutaneous Tu2449-HER2 glioma model (Figure S10). The confirmation with Tu2449 as a second glioblastoma model completely unrelated to the chemically induced GL261 model further supports our treatment approach. These results encourage as a next step to evaluate in future experiments the impact of combined therapy on survival and cure rates in an orthotopic intracranial glioblastoma model.

We employed anti-HER2.CAR/NK-92 cells derived from the human cell line NK-92 in the animal experiments, resulting in a xenogenic situation between human anti-HER2.CAR/NK-92 cells and murine resident immune cells. This could affect both, the cytokines released and direct ligand-receptor interactions, and hence represents a limitation of our experimental model. On the other hand, the anti-HER2.CAR/NK-92 cells are currently being tested in an early phase clinical trial,[12] and it appears important to test combination approaches with the potential to further enhance their clinical utility already with the clinical-grade product. To mitigate this limitation of the experimental model, species compatibility was ensured in *in vitro* experiments to the extent possible, and all key *in vitro* experiments were performed both with human and murine target cells.

Clinical trials exploring CAR-T cell therapies have shown in some instances severe neurotoxicity and organ toxicity, including in one case a fatal adverse event with trastuzumab-based HER2-specific CAR-T cells.[67] However, no such toxicity was observed with HER2-CAR T cells that used an FRP5-based antibody domain,[68] which targets a different HER2 epitope than trastuzumab and is the same employed in our study. In addition, both in our pre-clinical experiments and the ongoing CAR2BRAIN study, anti-HER2.CAR/NK-92 cells are applied locally via intratumoral or intracavitary injection, further reducing the risk for systemic toxicity. Accordingly, we did not observe any adverse effects in experimental animals in this and in previous studies.[5,35] In line with this, a recent study did not report cytokine release syndrome, neurotoxicity or graft-versus-host disease after CAR-NK cell therapy in leukemia and lymphoma patients, which are typical side effects of CAR-T cell therapy.[69]
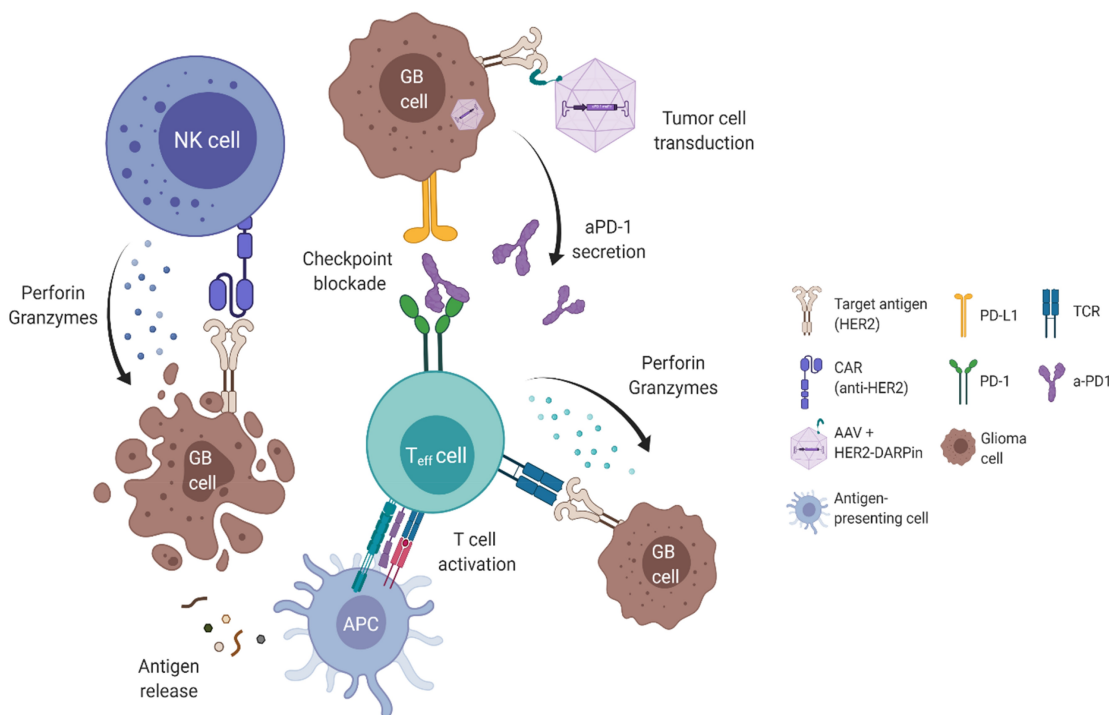

Figure 8. Potential synergism between anti-HER2.CAR/NK-92 cells and aPD-1 encoding HER2-AAV. Anti-HER2.CAR/NK-92 cell-mediated immune reactions against tumor cells can be inhibited by the immunosuppressive microenvironment. Upon selective transduction of HER2+ tumor cells, HER2-AAVaPD-1 induces local production of the aPD-1 checkpoint inhibitor. In combination with adoptively transferred anti-HER2.CAR/NK-92 cells, this may modify the immunosuppressive environment and facilitate a sustained anti-tumor immune response driven by endogenous immune cells.

We evaluated stability of HER2 expression in response to contact with anti-HER2.CAR/NK-92 cells and HER2-AAV transduction *in vitro*, but did not observe downregulation of the antigen as a possible escape mechanism in short term assays (Figure 5b and Figure S2e). In previous work from our group, also in glioblastoma mouse models no downregulation of HER2 after repetitive intratumoral anti-HER2.CAR/NK-92 cell injections was found.[5] In the same study, we further showed that HER2 expression is relatively stable in patients suffering from a glioblastoma relapse when compared to the initial primary tumor. We did not frequently detect antigen loss, as has been reported i.e. for EGFRvIII.[70]

Taken together, our data demonstrate that target-activated anti-HER2.CAR/NK-92 cells can induce upregulation of checkpoint molecules on neighboring tumor and immune cells, emphasizing the potential benefit of a combination therapy with an ICI-encoding HER2-AAV. The targeted AAV vector efficiently transduced tumor cells with high specificity, leading to secretion of functional aPD-1 and subsequent reactivation of T cells without affecting target antigen expression or interference with anti-HER2.CAR/NK-92 cell therapy. Hence, HER2-AAV^{aPD-1} can induce local secretion of the aPD-1 immunoadhesin by transduced tumor cells, which can modulate the immunosuppressive tumor microenvironment, support reactivation of T cells and thereby mediate synergistic effects when combined with adoptive transfer of anti-HER2.CAR/NK-92 cells (Figure 8). Moreover, in our study transduction of glioma cells by HER2-AAV *in vivo* resulted in high intratumoral but low systemic aPD-1 levels, and we did not observe immune-related side effects or toxicities upon administration of either the mono- or combination therapies. This may be pivotal to avoid systemic immune-related adverse events of combination immunotherapy and, together with the option to combine AAVs with different payloads, may provide an advantage over traditional systemic application of anti-PD-1 antibodies. The synergistic anti-tumor effect of anti-HER2.CAR/NK-92 cell therapy combined with HER2-AAV^{aPD-1} was demonstrated by pronounced tumor control and prolonged survival in the subcutaneous GL261-HER2 and reduced tumor growth in the Tu2449-HER2 glioma models. Taking all our findings into account, local therapy with HER2-AAV in combination with anti-HER2.CAR/NK-92 cells may represent a promising novel strategy for glioma immunotherapy with the potential to enhance efficacy and reduce side effects. Due to the high flexibility in AAV and CAR-NK cell target selection, as well as the choice of AAV payload, this type of immunotherapy has the potential to be customized for a particular type of malignant cells and the microenvironment of a specific tumor.

Acknowledgments

Disclosure statement

J.P.S has a consulting or advisory board membership with, or has received honoraria or travel or accommodation expenses from AbbVie, Medac, Novocure, Roche, and UCB. M.C.B has received honoraria for lectures or advisory board participation from Bristol-Myers Squibb and Gilead Sciences. All other authors report no conflict of interest.

Funding

ORCID

M.C. Burger (ID) http://orcid.org/0000-0002-6927-0987

Authors' contributions

M.C.B., C.J.B., J.P.S. and M.I.S. conceived the study and designed the experiments. M.I.S., K.W., F.S., B.R., G.L., S.K., T.A., C.O. and J.Rö. performed the experiments. M.I.S, M.C.B, K.W., F.S., B.R., L.S., C.O. and T.T. analyzed data. J.Re. and C.J.B. provided HER2-AAV vectors. J.Re. advised on vector constructs, aPD-1 ELISA and *in vivo* models. M.I.S. and M.C.B. wrote the manuscript. W.S.W. provided NK-92/5.28.z (anti-HER2.CAR-NK-92) cells and critical input. All authors helped to draft the manuscript and read and approved the final version.

References

1. Ohgaki H, Dessen P, Jourde B, Horstmann S, Nishikawa T, Di Patre P-L, Burkhard C, Schuler D, Probst-Hensch NM, Maiorka PC, et al. Genetic pathways to glioblastoma: a population-based study. Cancer Res. 2004 Oct;64(19):6892–6899. doi:10.1158/0008-5472.CAN-04-1337.

2. Stupp R, Mason WP, van den Bent MJ, Weller M, Fisher B, Taphoorn MJB, Belanger K, Brandes AA, Marosi C, Bogdahn U, et al. Radiotherapy plus concomitant and adjuvant temozolomide for glioblastoma. N Engl J Med. 2005;352(10):987–996. doi:10.1056/NEJMoa043330.

3. Cohen MH, Shen YL, Keegan P, Pazdur R. FDA drug approval summary: Bevacizumab (Avastin®) as treatment of recurrent glioblastoma multiforme. Oncologist. 2012 Nov;17(11):1482–1482. doi:10.1634/theoncologist.2009-0121erratum.

4. Schönfeld K, Sahm C, Zhang C, Naundorf S, Brendel C, Odendahl M, Nowakowska P, Bönig H, Köhl U, Kloess S, et al. Selective inhibition of tumor growth by clonal NK cells expressing an ErbB2/HER2-specific chimeric antigen receptor. Molecular Therapy. 2015 Feb;23(2):330–338. doi:10.1038/mt.2014.219.

5. Zhang C, Burger MC, Jennewein L, Genßler S, Schönfeld K, Zeiner P, Hattingen E, Harter PN, Mittelbronn M, Tonn T, Steinbach JP, Wels WS. ErbB2/HER2-Specific NK Cells for Targeted Therapy of Glioblastoma. J Natl Cancer Inst. 2015 Dec 6;108(5). doi:10.1093/jnci/djv375. PMID: 26640245.

6. Schlegel J, Stumm G, Brandle K, Merdes A, Mechtersheimer G, Hynes NE, Kiessling M. Amplification and differential expression of members of the erbB-gene family in human glioblastoma. J Neurooncol. 1994;22(3):201–207. doi:10.1007/BF01052920.

7. Andersson U, Guo D, Malmer B, Bergenheim AT, Brannstram T, Hedman H, Henriksson R. Epidermal growth factor receptor family (EGFR, ErbB2-4) in gliomas and meningiomas. Acta Neuropathol. 2004 Aug;108(2):135–142. doi:10.1007/s00401-004-0875-6.

8. Koka V, Potti A, Forseen SE, Pervez H, Fraiman GN, Koch M, Levitt R. Role of Her-2/neu overexpression and clinical determinants of early mortality in glioblastoma multiforme. Am J Clin

Oncol. 2003 Aug;26(4):332–335. doi:10.1097/01.COC.0000020922.66984.E7.

9. Liu G, Ying H, Zeng G, Wheeler CJ, Black KL, Yu JS. HER-2, gp100, and MAGE-1 are expressed in human glioblastoma and recognized by cytotoxic T cells. Cancer Res. 2004 Jul;64 (14):4980–4986. doi:10.1158/0008-5472.CAN-03-3504.

10. Human Proteome map. https://www.humanproteomemap.org/batch.php (accessed Nov. 13, 2021).

11. Burger MC, Mildenberger I, Zhang C, Ihrig K, Wagner M, Mittelbronn M, Senft C, Tonn T, Wels WS, Steinbach JP, et al. P04.05 The CAR2BRAIN study: a monocentric phase I trial with ErbB2-specific NK-92/5.28.z cells in recurrent glioblastoma. Neuro Oncol. 2016 Oct;18 (Suppl 4):iv24. doi:10.1093/NEUONC/NOW188.083.

12. Burger MC, Zhang C, Harter PN, Romanski A, Strassheimer F, Senft C, Tonn T, Steinbach JP, Wels WS. CAR-Engineered NK cells for the treatment of glioblastoma: turning innate effectors into precision tools for cancer immunotherapy. Frontiers in Immunology, 10. Frontiers Media S.A., Nov. 14, 2019. doi: 10.3389/fimmu.2019.02683.

13. Strassheimer F, Zhang C, Mildenberger IC, Harter PN, Tonn T, Steinbach JP, Wels WS, Burger MC. P04.21 Combination therapy of CAR-NK cells and anti-PD-1 antibody displays potent efficacy against late-stage Glioblastoma and induces protective antitumor immunity. Neuro Oncol. 2018 Sep;20(Suppl 3):iii283. doi:10.1093/NEUONC/NOY139.255.

14. Maki G, Klingemann HG, Martinson JA, Tam YK. Factors regulating the cytotoxic activity of the human natural killer cell line, NK-92. J Hematother Stem Cell Res. 2001;10(3):369–383. doi:10.1089/152581601750288975.

15. Kirwan SE, Burshtyn DN. Killer cell Ig-like receptor-dependent signaling by ig-like transcript 2 (ILT2/CD85j/LILRB1/LIR-1). The Journal of Immunology. 2005;175(8):5006–5015. doi:10.4049/jimmunol.175.8.5006.

16. Kloess S, Oberschmidt O, Dahlke J, Vu X-K, Neudoerfl C, Kloos A, Gardlowski T, Matthies N, Heuser M, Meyer J, et al. Preclinical assessment of suitable natural killer cell sources for chimeric antigen receptor natural killer-based 'off-the-shelf' acute myeloid leukemia immunotherapies. Hum Gene Ther. 2019;30(4):381–401. doi:10.1089/hum.2018.247.

17. Gong JH, Maki G, Klingemann HG. Characterization of a human cell line (NK-92) with phenotypical and functional characteristics of activated natural killer cells. Leukemia. 1994 Apr;8(4):652-8. PMID: 8152260.

18. Tonn T, Schwabe D, Klingemann HG, Becker S, Esser R, Koehl U, Suttorp M, Seifried E, Ottmann OG, Bug G, et al. Treatment of patients with advanced cancer with the natural killer cell line NK-92. Cytotherapy. 2013 Dec;15(12):1563–1570. doi:10.1016/J.JCYT.2013.06.017.

19. Nowakowska P, Romanski A, Miller N, Odendahl M, Bonig H, Zhang C, Seifried E, Wels WS, Tonn T. Clinical grade manufacturing of genetically modified, CAR-expressing NK-92 cells for the treatment of ErbB2-positive malignancies. Cancer Immunol Immunother. 2018 Jan;67(1):25–38. doi:10.1007/S00262-017-2055-2.

20. Klingemann H, Boissel L, Toneguzzo F. Natural killer cells for immunotherapy – advantages of the nk-92 cell line over blood NK cells. Front Immunol. 2016 Mar;(MAR):91. doi:10.3389/FIMMU.2016.00091.

21. Wang L, Ge J, Lan Y, Shi Y, Luo Y, Tan Y, Liang M, Deng S, Zhang X, Wang W, Tan Y, Xu Y, Luo T. Tumor mutational burden is associated with poor outcomes in diffuse glioma. BMC Cancer. 2020 Mar 12;20(1):213. doi:10.1186/s12885-020-6658-1. PMID: 32164609; PMCID: PMC7069200.

22. Nduom EK, Weller M, Heimberger AB. Immunosuppressive mechanisms in glioblastoma. Neuro Oncol. 2015;17 Suppl 7 (suppl 7):vii9–vii14. doi:10.1093/neuonc/nov151.

23. Wintterle S, Schreiner B, Mitsdoerffer M, Schneider D, Chen L, Meyermann R, Weller M, Wiendl H. Expression of the B7-related molecule B7-H1 by glioma cells: a potential mechanism of immune paralysis.," Cancer Res. 2003 Nov 1;63(21):7462–7467. PMID: 14612546.

24. Bloch O, Crane CA, Kaur R, Safaee M, Rutkowski MJ, Parsa AT. Gliomas promote immunosuppression through induction of B7-H1 expression in tumor-associated macrophages. Clin Cancer Res. 2013;19(12):3165–3175. doi:10.1158/1078-0432.CCR-12-3314.

25. Cloughesy TF, Mochizuki AY, Orpilla JR, Hugo W, Lee AH, Davidson TB, Wang AC, Ellingson BM, Rytlewski JA, Sanders CM, et al. Neoadjuvant anti-PD-1 immunotherapy promotes a survival benefit with intratumoral and systemic immune responses in recurrent glioblastoma. Nat Med. 2019 Mar;25 (3):477–486. doi:10.1038/S41591-018-0337-7.

26. Reardon DA, Brandes AA, Omuro A, Mulholland P, Lim M, Wick A, Baehring J, Ahluwalia MS, Roth P, Bähr O, et al. Effect of nivolumab vs bevacizumab in patients with recurrent glioblastoma: the checkmate 143 phase 3 randomized clinical trial. JAMA Oncol. 2020 Jul;6(7):1003–1010. doi:10.1001/JAMAONCOL.2020.1024.

27. Weber JS, Kähler KC, Hauschild A. Management of immune-related adverse events and kinetics of response with ipilimumab. J Clin Oncol. 2012 Jul;30(21):2691–2697. doi:10.1200/JCO.2012.41.6750.

28. Reul J, Frisch J, Engeland CE, Thalheimer FB, Hartmann J, Ungerechts G, Buchholz CJ. Tumor-specific delivery of immune checkpoint inhibitors by engineered AAV vectors. Front Oncol. 2019 Feb;9:52. doi:10.3389/fonc.2019.00052.

29. Verdera HC, Kuranda K, Mingozzi F. AAV vector immunogenicity in humans: a long journey to successful gene transfer. Mol Ther. 2020 Mar;28(3):723–746. doi:10.1016/J.YMTHE.2019.12.010.

30. Büning H, Huber A, Zhang L, Meumann N, Hacker U. Engineering the AAV capsid to optimize vector-host-interactions. Curr Opin Pharmacol. 2015 Oct;24:94–104. doi:10.1016/J.COPH.2015.08.002.

31. Münch RC, Janicki H, Völker I, Rasbach A, Hallek M, Büning H, Buchholz CJ. Displaying high-affinity ligands on adeno-associated viral vectors enables tumor cell-specific and safe gene transfer. Molecular Therapy. 2013 Jan;21(1):109–118. doi:10.1038/mt.2012.186.

32. Münch RC, Muth A, Muik A, Friedel T, Schmatz J, Dreier B, Trkola A, Plückthun A, Büning H, Buchholz CJ, et al. Off-target-free gene delivery by affinity-purified receptor-targeted viral vectors. Nat Commun. 2015 Dec;6(1):6246. doi:10.1038/ncomms7246.

33. Steinbach JP, Klumpp A, Wolburg H, Weller M. Inhibition of epidermal growth factor receptor signaling protects human malignant glioma cells from hypoxia-induced cell death. Cancer Res. 2004 Mar;64(5):1575–1578. doi:10.1158/0008-5472.CAN-03-3775.

34. Sonoda Y, Ozawa T, Hirose Y, Aldape KD, McMahon M, Berger MS, Pieper RO. Formation of intracranial tumors by genetically modified human astrocytes defines four pathways critical in the development of human anaplastic astrocytoma. Cancer Res. 2001 Jul;61(13):4956–4960.

35. Genßler S, Burger MC, Zhang C, Oelsner S, Mildenberger I, Wagner M, Steinbach JP, Wels WS. Dual targeting of glioblastoma with chimeric antigen receptor-engineered natural killer cells overcomes heterogeneity of target antigen expression and enhances antitumor activity and survival. Oncoimmunology. 2015 Dec 21;5(4):e1119354. doi:10.1080/2162402X.2015.1119354. PMID: 27141401; PMCID: PMC4839317.

36. Sahm C, Schönfeld K, Wels WS. Expression of IL-15 in NK cells results in rapid enrichment and selective cytotoxicity of gene-modified effectors that carry a tumor-specific antigen receptor. Cancer Immunol Immunother. 2012 Sep;61 (9):1451–1461. doi:10.1007/S00262-012-1212-X.

37. Steinbach JP, Wolburg H, Klumpp A, Probst H, Weller M. Hypoxia-induced cell death in human malignant glioma cells: energy deprivation promotes decoupling of mitochondrial cytochrome c release from caspase processing and necrotic cell death. Cell Death & Differentiation. 2003 Jun;10(7):823–832. doi:10.1038/sj.cdd.4401252.

38. Chae WH, Niesel K, Schulz M, Klemm F, Joyce JA, Prümmer M, Brill B, Bergs J, Rödel F, Pilatus U, et al. Evaluating magnetic resonance spectroscopy as a tool for monitoring therapeutic response of whole brain radiotherapy in a mouse model for breast-to-brain metastasis. Front Oncol, vol. 9, Nov. 2019, doi:10.3389/FONC.2019.01324.

39. Pohl U, Wick W, Weissenberger J, Steinbach JP, Dichgans J, Aguzzi A, Weller M. Characterization of Tu-2449, a glioma cell line derived from a spontaneous tumor in GFAP-v-src-transgenic mice: comparison with established murine glioma cell lines. Int J Oncol. 1999 Oct;15(4):829-34. doi:10.3892/ijo.15.4.829. PMID: 10493969.

40. Myers JA, Miller JS. Exploring the NK cell platform for cancer immunotherapy. Nat Rev Clin Oncol. 2021 Feb;18(2):85–100. doi:10.1038/S41571-020-0426-7.

41. Lin G, Wang J, Lao X, Wang J, Li L, Li S, Zhang J, Dong Y, Chang AE, Li Q, et al. Interleukin-6 inhibits regulatory T cells and improves the proliferation and cytotoxic activity of cytokine-induced killer cells. J Immunother. 2012 May;35 (4):337–343. doi:10.1097/CJI.0B013E318255ADA3.

42. Kimura A, Kishimoto T. IL-6: regulator of Treg/Th17 balance. Eur J Immunol. 2010 Jul;40(7):1830–1835. doi:10.1002/EJI.201040391.

43. Vivier E, Raulet DH, Moretta A, Caligiuri MA, Zitvogel L, Lanier LL, Yokoyama WM, Ugolini S. Innate or adaptive immunity? The example of natural killer cells. Science. 2011 Jan;331 (6013):44–49. 2011. doi:10.1126/SCIENCE.1198687.

44. Cook KD, Waggoner SN, Whitmire JK. NK cells and their ability to modulate T cells during virus infections. Critical Reviews™ in Immunology. 2014;34(5):359–388. doi:10.1615/CRITREVIMMUNOL.2014010604.

45. Blanchard DK, Michelini-Norris M, Pearson CA, McMillen S, Djeu JY. Production of granulocyte-macrophage colony-stimulating factor (GM-CSF) by monocytes and large granular lymphocytes stimulated with Mycobacterium avium-M. intracellulare: activation of bactericidal activity by GM-CSF. Infect Immun. 1991;59 (7):2396–2402. doi:10.1038/mt.2014.219.

46. van den Bosch G, Preijers F, Vreugdenhil A, Hendriks J, Maas F, De Witte T. Granulocyte-macrophage colony-stimulating factor (GM-CSF) counteracts the inhibiting effect of monocytes on natural killer (NK) cells. Clin Exp Immunol. 2008 Sep;101(3):515–520. doi:10.1111/J.1365-2249.1995.TB03143.X.

47. Walzer T, Dalod M, Robbins SH, Zitvogel L, Vivier E. Natural-killer cells and dendritic cells: 'l'union fait la force,'. Blood. 2005 Oct;106(7):2252–2258. doi:10.1182/BLOOD-2005-03-1154.

48. Francisco LM, Sage PT, Sharpe AH. The PD-1 pathway in tolerance and autoimmunity. Immunol Rev. 2010 Jul;236(1):219–242. doi:10.1111/J.1600-065X.2010.00923.X.

49. Broekman ML, Maas SLN, Abels ER, Mempel TR, Krichevsky AM, Breakefield XO. Multidimensional communication in the microenvirons of glioblastoma. Nat Rev Neurol. 2018 Jul;14(8):1–14. doi:10.1038/S41582-018-0025-8.

50. Parsa AT, Waldron JS, Panner A, Crane CA, Parney IF, Barry JJ, Cachola KE, Murray JC, Tihan T, Jensen MC, et al. Loss of tumor suppressor PTEN function increases B7-H1 expression and immunoresistance in glioma. Nat Med. 2007;13(1):84–88. doi:10.1038/nm1517.

51. Qian J, et al. The IFN-γ/PD-L1 axis between T cells and tumor microenvironment: hints for glioma anti-PD-1/PD-L1 therapy. J Neuroinflammation. 1979 Oct;15(1):1–13. 2018. doi:10.1186/S12974-018-1330-2.

52. Berghoff AS, Kiesel B, Widhalm G, Rajky O, Ricken G, Wöhrer A, Dieckmann K, Filipits M, Brandstetter A, Weller M, et al. Programmed death ligand 1 expression and tumor-infiltrating lymphocytes in glioblastoma. Neuro Oncol. 2015 Aug;17 (8):1064–1075. doi:10.1093/neuonc/nou307.

53. Natajaran A, Mayer AT, Xu L, Reeves RE, Gano J, Gambhir SS. Novel radiotracer for immunoPET imaging of PD-1 checkpoint expression on tumor infiltrating lymphocytes. Bioconjug Chem. 2015 Oct;26(10):2062–2069. doi:10.1021/ACS.BIOCONJCHEM.5B00318.

54. Fuchs SP, Desrosiers RC. Promise and problems associated with the use of recombinant AAV for the delivery of anti-HIV antibodies. Mol Ther Methods Clin Dev. 2016 Jan;3:16068. doi:10.1038/MTM.2016.68.

55. Smith RH. Adeno-associated virus integration: virus versus vector. Gene Ther. 2008 Jun;15(11):817–822. doi:10.1038/GT.2008.55.

56. Schnepp BC, Chulay JD, Ye G-J, Flotte TR, Trapnell BC, Johnson PR. Recombinant adeno-associated virus vector genomes take the form of long-lived, transcriptionally competent episomes in human muscle. Hum Gene Ther. 2016 Jan;27(1):32–42. doi:10.1089/HUM.2015.136.

57. Naidoo J, Cottrell TR, Lipson EJ, Forde PM, Illei PB, Yarmus LB, Voong KR, Feller-Kopman D, Lee H, Riemer J, et al. Chronic immune checkpoint inhibitor pneumonitis. J Immunother Cancer. 2020 Jun;8(1):e000840. doi:10.1136/JITC-2020-000840.

58. Sorkin A, Goh LK. Endocytosis and intracellular trafficking of ErbBs. Exp Cell Res. 2009 Feb;315(4):683–696. doi:10.1016/J.YEXCR.2008.07.029.

59. Shilova ON, Proshkina GM, Lebedenko EN, Deyev SM. Internalization and recycling of the HER2 receptor on human breast adenocarcinoma cells treated with targeted phototoxic protein DARPinminiSOG. Acta Naturae. 2015;7(3):126. doi:10.32607/20758251-2015-7-3-126-132.

60. Hinderer C, Katz N, Buza EL, Dyer C, Goode T, Bell P, Richman LK, Wilson JM. Severe toxicity in nonhuman primates and piglets following high-dose intravenous administration of an adeno-associated virus vector expressing human SMN. Hum Gene Ther. 2018 Mar;29(3):285–298. doi:10.1089/HUM.2018.015.

61. Li C, Narkbunnam N, Samulski RJ, Asokan A, Hu G, Jacobson LJ, Manco-Johnson MJ, Monahan PE. Neutralizing antibodies against adeno-associated virus examined prospectively in pediatric patients with hemophilia. Gene Therapy. 2012 Mar;19 (3):288–294. doi:10.1038/GT.2011.90.

62. Calcedo R, Morizono H, Wang L, McCarter R, He J, Jones D, Batshaw ML, Wilson JM. Adeno-associated virus antibody profiles in newborns, children, and adolescents. Clin Vaccine Immunol. 2011 Sep;18(9):1586–1588. doi:10.1128/CVI.05107-11.

63. Rapti K, Louis-Jeune V, Kohlbrenner E, Ishikawa K, Ladage D, Zolotukhin S, Hajjar RJ, Weber T. Neutralizing antibodies against AAV serotypes 1, 2, 6, and 9 in sera of commonly used animal models. Mol Ther. 2012 Jan;20(1):73–83. doi:10.1038/mt.2011.177.

64. Bartel M, Schaffer D, Büning H. Enhancing the clinical potential of AAV vectors by capsid engineering to evade pre-existing immunity. Front Microbiol. 2011;(OCT):204. doi:10.3389/FMICB.2011.00204.

65. Asokan A, Schaffer DV, Samulski RJ. The AAV vector toolkit: poised at the clinical crossroads. Molecular Therapy. 2012 Apr;20 (4):699–708. doi:10.1038/MT.2011.287.

66. Xu J, Zhang J, Xin L, Yang C, Zhang F, Tang S, Yao J, Wang H, Qinjie N, Yan M, et al. Prevalence of neutralizing antibodies against AAV8, AAV9, and AAV843 in a Chinese population. Int J Clin Exp Med. 2019;12(8):10253–10261.

67. Morgan RA, Yang JC, Kitano M, Dudley ME, Laurencot CM, Rosenberg SA. Case report of a serious adverse event following the administration of T cells transduced with a chimeric antigen receptor recognizing ERBB2. Mol Ther. 2010 Apr;18(4):843–851. doi:10.1038/MT.2010.24.

68. Ahmed N, Brawley VS, Hegde M, Robertson C, Ghazi A, Gerken C, Liu E, Dakhova O, Ashoori A, Corder A, et al. Human epidermal growth factor receptor 2 (HER2) –specific chimeric antigen receptor–modified T cells for the immunotherapy of HER2-positive sarcoma. J Clin Oncol. 2015 May;33(15):1688–1696. doi:10.1200/JCO.2014.58.0225.

69. Liu E, Marin D, Banerjee P, Macapinlac HA, Thompson P, Basar R, Nassif Kerbauy L, Overman B, Thall P, Kaplan M, et al. Use of CAR-transduced natural killer cells in CD19-positive lymphoid tumors. New England Journal of Medicine. 2020;382(6):545–553. doi:10.1056/nejmoa1910607.

70. Eskilsson E, Røsland GV, Solecki G, Wang Q, Harter PN, Graziani G, Verhaak RGW, Winkler F, Bjerkvig R, Miletic H, et al. EGFR heterogeneity and implications for therapeutic intervention in glioblastoma. Neuro Oncol. 2018;20(6):743–752. doi:10.1093/neuonc/nox191.